4-2008

Effect of High Temperature Drying of Paper on Heat Transfer Rates and Sheet Properties

Dania Awni Al-Said

EFFECT OF HIGH TEMPERATURE DRYING OF PAPER ON HEAT TRANSFER RATES AND SHEET PROPERTIES

by

Dania Awni Al-Said

A Thesis
Submitted to the
Faculty of the Graduate College
in partial fulfillment of the
requirements for the
Degree of Master of Science
Department of Paper Engineering, Chemical Engineering, and Imaging

Western Michigan University
Kalamazoo, MI
April 2008

ACKNOWLEDGEMENTS

Many thanks and much gratitude to my beloved parents and family, for their encouragement and unlimited support. I will always be grateful for their enthusiasm, guidance and love. I would like to express my warmest gratitude and special thanks to my husband, Hasan, and my beautiful children Jude and Ahmad, for their patience and support. It is because of them that I completed this thesis. I love them more than words can say.

My sincere appreciation goes to my major advisor, Dr. John Cameron, for his supervision and assistance during my research work and studies. I would like to acknowledge him for the stimulating discussions we had.

I would like to thank the members of my sponsoring committee, Dr. Said Abubakr and Dr. Andy Kline. Thank you for agreeing to serve on my thesis committee despite your busy schedules. Thank you for all your help and encouragement. Your support is appreciated.

To the faculty whom I had classes with, or the opportunity to work with, or know during the last two years, thanks for the memories.

Dania Awni Al-Said

EFFECT OF HIGH TEMPERATURE DRYING OF PAPER ON HEAT TRANSFER RATES AND SHEET PROPERTIES

Dania Awni Al-Said, M.S.

Western Michigan University, 2008

The objective of this research is to study the effect of high temperature on paper drying rates and properties of both virgin pulp and recycled paper. Process variables as shell temperature, moisture content, refining, basis weight and fiber recycling can affect the drying rate and paper properties. In addition, high surface temperature can affect the heat transfer rates from the dryer shell to the paper. The Gas Heated Paper Dryer (GHPD) is a high temperature dryer where internal shell temperature can reach 300° C, which significantly increases the drying rate. However, there are many concerns about the effect of this high temperature on paper properties especially paper curl and paper strength.

In this research, a laboratory drying system that simulates paper drying at elevated temperatures was used to dry different handsheets. The heat transfer coefficient was found to be constant in the constant rate drying zone and in the first following rate zone, but decreased with an increase in shell temperature in the second following rate zone. This result provided information that optimizes the location of the high temperature dryer. At the ideal location, the heat transfer and drying rates are maximized with minimum effects on sheet properties. Sheet curl was found to be a function of recycling and the drying temperature.

TABLE OF CONTENTS

Table Of Contents- Continued

LIST OF TABLES

LIST OF FIGURES

List Of Figures-Continued

PROBLEM STATEMENT

Paper drying is the most expensive section in a paper mill in the capital and operating costs for the high-energy consumption. It consumes about 85% of the heat energy used in papermaking [1]. The conventional drying cylinder is the dominant method for paper drying. Steam is supplied to the cylinders as the energy source. As steam condenses in the inner surface of the cylinder, latent heat of vaporization is released and heat is transferred to the paper [2]. In a typical modern machine, 1 kg of water requires 1.3 kg of steam to evaporate [3]. The mass of steam per unit mass of water evaporated or the thousands of (BTUs) per pound of water evaporated (or kJ/kg) are measurements of steam economy [3]. The typical steam energy consumption for steam cylinders is 1,275 to 1,575 BTUs steam input per pound of water evaporated from the sheet [4].

Because of this high-energy consumption for water evaporation, the drying process requires effective heat transfer from the dryer cylinders to the paper. In addition to energy consumption, the dryer capacity limits the machine speed and the production rates [5]. Therefore, the drying section should be as economical and effective as possible while maintaining the required paper properties [6]. Recently, there has been considerable interest in increasing the rate of paper drying to increase production rate. The Gas Fired Paper Dryer GFPD (high temperature drying) is one method to increase the drying rate where one or more conventional dryers are replaced with this gas-fired equipment. The gas-fired dryer can provide internal shell temperatures up to 300 °C [7], which significantly increases the drying rate. However, several issues should be taken into consideration with any installation. These include; the effect of high shell temperature on the drying rate, the contact coefficient and paper properties.

This research studied the effect of high shell temperature and one side drying on drying rates, shell-paper contact coefficients and paper properties. In addition, the study examined other process variables from recycling, refining, basis weight and moisture content. The results were analyzed by MINITAB Release 14.1 to determine the significant variable.

LITERATURE REVIEW

Cylinder Dryers

Paper machines usually have 3 to 5 drying sections. Each section has around 6 to 16 drying cylinders between 1.5 to 2.2 m in diameter [8]. A permeable fabric called dryer felt holds the web while drying. Steam is supplied into these cylinders at saturation temperature. As heat transfers from the steam cylinder to the wet web, steam condenses at a temperature defined by the pressure in the system [9]. The condensate formed in the cylinders is then removed for heat recovery by heat exchangers. In modern machines, the drying section is totally enclosed by a hood where hot air is supplied to carry away water vapor produced by drying to heat recovery or exhaust [10].

The dryer fabric or sometimes called the felt supports the sheet and restrain the movement of the sheet that shrinks in the cross direction (CD) while drying [11]. In addition, the dryer fabric keeps the sheet flat and free from wrinkles while drying.

The surface temperature achieved by steam cylinders is limited by the pressure rating of the cylinders [9]. Due to ASTM pressure codes, the steam pressure is limited to 160 psig, which limits the internal shell temperature to the steam condensing temperature at this pressure [5]. Figure 1 shows an example of TAPPI drying rates' chart. The diagram illustrates the effect of the steam pressure and condensing temperature inside the drying cylinders on the drying rates. The middle line in the diagram shows the average performance of a machine producing specific grade of paper [12]. The figure shows the maximum steam condensing temperature in cylinder dryer to be about 300 °F, which is around 149 °C.

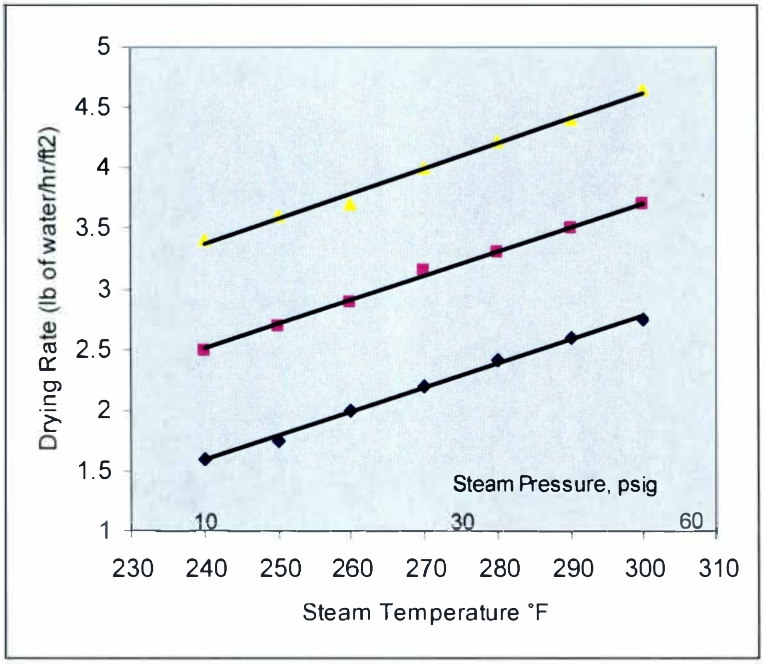

Figure 1. Steam Temperature in Dryer Cylinders Adapted From [11].

To overcome the limitation of surface temperature and hence drying rates of steam cylinders, a great interest and research were combined to develop high drying rate equipments and technologies. The Gas Heated Paper Dryer (GHPD) is one method to increase the drying rate [5]. Gas combustion is the heating source in this equipment instead of steam [13]. The GHPD eliminates the need for pressurizing the cylinder to obtain higher surface temperature while drying [13]. Higher shell temperatures assist the heat transfer process to achieve higher drying rates that help the paper industry increase the production rate from dryer-limited paper machine [5]. In the commercial application of GHPD, the surface temperatures can reach 300 °C under atmospheric pressure with no negative effect on paper properties [7]. The

GFPD minimizes the steam consumption and provides an increase in energy efficiency from 65% (steam operated) to 75-80% (gas operated) [5]. Additional to the energy savings, significant capital costs savings are expected for both retrofit and new installations [5].

The gas-fired alternatives were developed by British Gas [14], ABB Drying [15] and Gastec NV [16]. The ABB design was the only approach introduced to the commercial market. The commercialized concept utilized a radiative heat transfer source to heat the dryer surface [5].

The need for frequent maintenance of radiant burners makes them less efficient than convective heat transfer applications [5]. Since the convective heat transfer is more efficient and cost effective, the Gas Technology Institute (GTI) initiated the development of an innovative approach to natural gas-fired dryer. In this approach, both radiant and convective heat transfer are accomplished [18]. The institute selected a Flynn's ribbon burner (model T-534) to provide a sheet flow of natural gas combustion products along the drying drum surface [5]. Natural gas is injected into small dimples or cavities in this dryer and the combustion air is supplied from the outside and normal to these dimples to create air vortices. These vortices create mini flames to obtain uniform surface temperature. The expected dryer efficiency in this approach is higher than the drying rates attained by the conventional system with low emission of NO_x gases [18].

GFPD is an effective method to increase the drying rates where one or more conventional dryers are replaced with this gas-fired dryer without major modification to the paper drying section and without any need for the pressure vessel in the dryer drum [5, 13]. In addition, the application offers a wide range of surface temperatures by controlling the combustion process [19,20].

When paper dries, it goes through different drying phases or zones. The first zone is the warm up zone, where the evaporation rate and web temperature rise continuously [21]. The second zone is the constant rate zone where evaporation quickly reaches the maximum rate [11] and the heat transfer from the cylinder to the web determines the drying rate [22]. The third zone is the falling rate zone where the moisture is concentrated in smaller capillaries [11]. In this zone, the surface of the web is partly dry and its heat conductivity decreases. The drying rate and the energy used for evaporation start decreasing [21]. Therefore, the web temperature begins to rise for the energy balances [21]. The falling rate zone is divided into two zones: the first falling rate zone and the second falling rate zone. The second falling rate zone is called sometimes the bound water zone. This zone begins when all the free water evaporates and physicochemical forces -that are hard to break- hold the remaining water [11, 23]. Figure 2 illustrates these different drying zones and the changes in the web temperature as the drying proceeds.

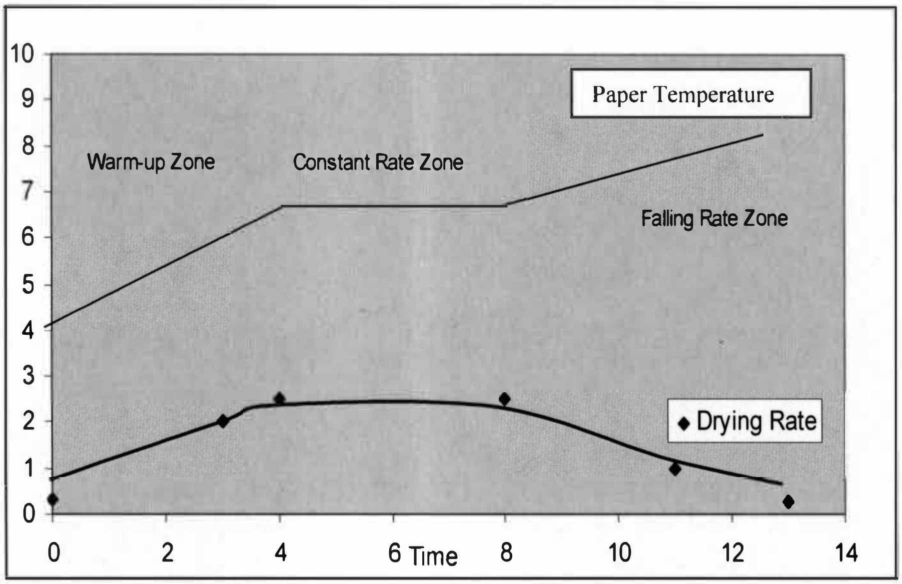

Figure 2. Paper Drying Zones Adapted From [24].

The thermal energy necessary for heating the dryer cylinders is obtained from steam condensation. As steam condenses, it releases its latent heat of vaporization [2]. When the paper web contacts the cylinder, the temperature gradient between the two surfaces assists the heat transfer process [25]. This heat flow meets thermal resistances from the inner surface of the cylinder until it reaches the paper surface. These resistances are the condensate layer in the inner side of the dryer cylinder, the scale, the cylinder shell, the shell-paper contact resistance and the paper web [2]. Figure 3 illustrates schematically the heat transfer from the steam through the shell to the paper and the individual resistance components.

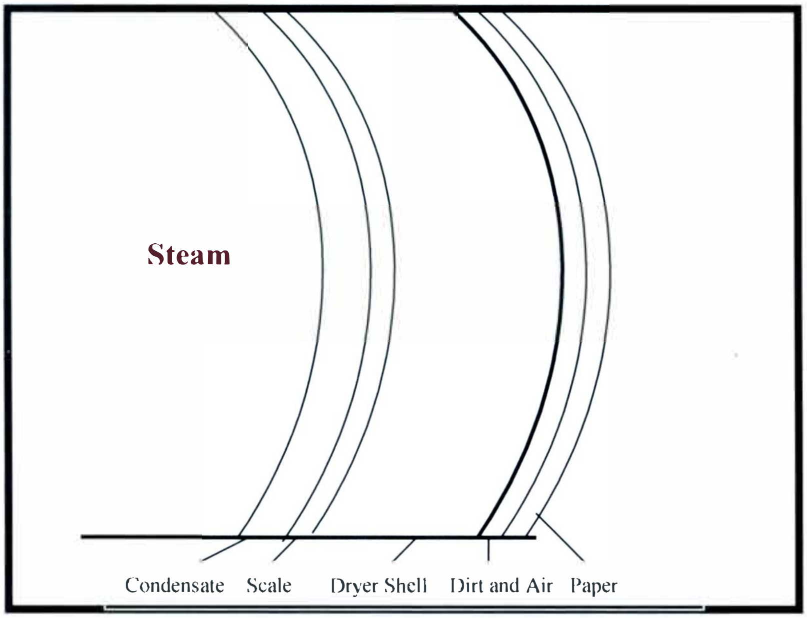

Figure 3. Heat Transfer Resistances from Steam to Paper Adapted From [26].

The primary metal used in cylinder dryers is cast iron with high thermal conductivity. The typical thickness range of the shell is 25 to 38mm [2]. Many tests and calculations showed that the total heat transfer does not improve with thinner shells and that the thermal conductivity is usually lower in thinner, strong materials. In addition, it is difficult to ensure roundness in a thin-wall dryer [2].

The last resistance to heat transfer is in the paper web as in figure 6. The heat transfers and accumulates through the paper thickness. The paper web resistance is less important and has less effect on the total heat transfer especially for lightweight grades [2].

The most important resistance for heat transfer is at the interface between the cylinder shell and paper surface. Due to the roughness of both surfaces, there are areas with gas-filled gaps that will resist the heat transfer [27]. Around 35-70% of the total heat resistance in paper drying is encountered at the paper-shell contact surface

[28]. This resistance is the paper-shell contact coefficient from the cylinder to web and it is defined as in equation (1) [27]:

$$\alpha_k = \frac{q}{T_{c2} - T_{pi}} \qquad (1)$$

Where α_k Is the contact coefficient (W/m^2.°C)

q Is the heat flux (W/m^2). The area here is the contact area between the web and cylinder.

T_{c2} Is the temperature of the dryer outer surface.

T_{pi} Is the temperature of the paper surface against the cylinder.

The paper-shell contact coefficient is the most critical resistance to heat transfer and the majority of the experimental studies [28, 29] on paper drying have focused on studying this parameter. These studies can be divided into static bench-scale experiments, dynamic lab-scale experiments and dynamic full-scale experiments [28]. While the third study may seem more reliable, the first and second experiments provide many advantages. The major advantages are the ease of changing the drying parameters to obtain different conditions, the rapid drying data collection and analysis [28].

The contact coefficient value is important and is affected by many factors such as the shell temperature [30], paper moisture content [27], basis weight, fiber refining and recycling. The following explains the effect of these factors on the contact coefficient.

Shell Temperature

The shell temperature has a great effect on the heat transfer and the contact coefficient. The literature shows that this effect of shell temperature on the contact coefficient is under a great investigation. For example, Wilhelmsson, *et al.* [28] found that an increase in surface temperature results in a substantial increase in the contact coefficient. This temperature dependence of the contact coefficient is supported by the results of Redfern [30]. Other studies have reported conflicting results of the effect of higher surface temperature on the contact coefficient. Poirier [13] found that the contact coefficient decreases as the shell temperature increases. He explained his found that the increased drying rate creates a vapor film that reduces the contact coefficient especially when the film cannot pass through the web pores and channels. Poirier's drying rates were not straight lines which is explained by the reduction in the contact coefficient at elevated temperatures [13].

Paper Moisture Content

Moisture content (Z_{mc}) is the amount of water in a paper web or pulp suspension. It is defined as in equation (2) [31]:

$$Z_{mc} = \frac{m_w}{m_d + m_w} .100\% \qquad (2)$$

Where m_w is the mass of water

m_d is the mass of the dry material

The expression of moisture content sometimes uses the mass of water to the dry material (z_{mr}) as in equation (3) [31]:

$$z_{mr} = \frac{m_w}{m_d} \quad (3)$$

After pressing, the wet paper enters the drying section at a moisture content between 65% and 50% in moist basis [8] which is about 35 and 50% dryness. At the end of drying, the moisture content for the output sheet is in the range 3.5% to 9% depending on the paper grade and composition [8].

The majority of the contact coefficient studies found that it is highly dependent on the water/solids ratio of the paper. For example, the measurement of Hinds, and Neogi showed that the contact coefficient decreased as web moisture decreased [32]. The same found was obtained by Wilhelmsson, *et al.* [28] where the contact coefficient decreased from about 800 $W/m^{2o}C$ to 200 $W/m^{2o}C$ as the moisture ratio in the paper decreased from 1.0 g-water/g-solids to 0.2 g-water/g-solids. A logical explanation is that direct water to cylinder contact exists when the paper surface is wet [27]. As drying proceeds, this contact is no longer present which lowers the heat transfer and the drying rates.

The results of Cameron [34] showed that the reduction in the contact coefficient is a linear function of the moisture ratio in the falling rate zone of paper drying and shell surface temperature lower than 150˚C. Above this temperature and at moisture ratios greater than 1.0 g water/g oven dried fibers, the heat transfer was rapid until a vapor film was formed and reduced the drying rates at that point [34].

Paper Recycling

The major effect of recycling on the fiber is the reduction of water bound to the cellulose and hemicellulose [35] and the water swelling of wood fibers [36]. Cameron [35] found that recycling reduces the fiber surface area available for sorption which reduces the point where the falling rate period begins and hence should reduce the over all drying time. However, little information is available in the literature on the effect of fiber recycling on the contact coefficient.

Paper Basis Weight

Lang, *et al.* [7] found that the high temperature drying rates of newsprint and fine paper are greater than those of linerboard and corrugated medium. This increase in the drying rate is important in predicting the possible production increase with higher drying temperatures.

Drying and Paper Properties

In setting the cylinder temperature, the need for higher evaporation rates is balanced against the effect on paper properties. After the drying section, the basic requirement in paper property is the uniformity of the moisture profile –in the cross machine direction CD- that affects paper shrinkage and paper curl [37].

Paper Shrinkage

In laboratory handsheets, fibers orients randomly at no preferred direction and measured properties are isotropic in the plane of the sheet [38]. When the sheet enters the drying section, the contact surface of the wet web is heated to the water boiling temperature or about 100 ˚C. The water starts evaporating and leaves the structure to the outer surface of the paper [25]. As water evaporates, the capillary forces draw the swollen fibers and any loosened fibrils –due to refining- to the wall materials. Then hydrogen bonds between the hydroxyl groups hold the structure together. This causes fiber shrinkage where pores close and fibers form a network with internal stresses [38].

While fibers shrink primary in the lateral direction, the longitudinal stiffness of fibers competes against this lateral shrinkage. This imposition between the lateral and the longitudinal compression at the bond site creates what is called "microcompressions" [38, 39].

The microcmpression theory is very important and affects greatly several paper properties. It also explains how the almost exclusively (or dominant) lateral shrinkage of the fibers during drying produces sheet shrinkage in all directions [38]. However, in commercial paper drying, the fibers shrink more in the machine CD since the lateral shrinkage is higher than longitudinal and fibers are oriented in the MD. In addition, the stress applied in the MD during drying controls web shrinkage in this direction [39].

The shrinkage potential of mechanical pulp paper is smaller than in chemical pulp. Chemical pulp dissolves most of the lignin so that the wall structure is more porous and penetrable by water than mechanical pulp [37]. Chemical pulp responds more to post refining which causes more swelling and higher fiber shrinkage while drying. Refining and fiber fibrillation influence the point where paper starts to shrink. A paper made of strongly refined pulp starts to shrink when drying freely at 70%-80% moisture content, while paper made from non-beaten pulp starts to shrink at 50-60% moisture content [37].

Paper Curl

Curl is deviation from flatness as a result of non-uniform shrinkage of the paper which is caused mainly by the difference in fiber orientation through the thickness of the paper [40]. Stressing and drying of paper are other factors that have significant effect on paper curl [41]. The non-uniform water evaporation between the bottom side against the dryer cylinder and the top side causes paper to curl while drying. The side that dries first is under tension and cannot shrink after drying [40]. As drying proceeds, the wetter side continues to lose moisture and shrink with higher internal stresses [40, 41]. For printing grades, curl and shrinkage are usually away from the heated surface [40]. For thicker grades like boards, curl is a result of a moisture gradient in the z-direction due to hysteresis. The side against the hotter cylinders dries last and shrinks more which causes board to curl toward the hotter surface [40].

Controlling the drying rate of both sides of the web helps controlling paper curl [40]. In a commercial drier, the bottom cylinder counteracts the curl obtained from the top cylinder. This is true when both cylinders have similar shell temperatures. If the shell temperature of one of the cylinders is higher, the web will curl toward the hotter surface [40].

The temperature level of the cylinder shell is another factor that can influence paper curl [42]. Static experiment done by Siegel [42] showed the tendency of paper to curl at temperatures above 110°C.

Strength Properties

In the dryer section, the web conditions from temperature, moisture content and state of stresses have a significant effect on paper final properties. During paper drying, the moisture content at about 40 to 50% is called the critical moisture content. After this point, water is removed from the lumen and fibers collapse and shrink. This shrinkage brings the fibers close to each other to form hydrogen bonds [43]. Therefore, the strength of the web increases strongly until the paper reaches the final dryness level. Both the strength of the hydrogen bonds and the amount of the bonded area determine the strength properties of the paper [43].

As the drying proceeds, the solid content increases and hydrogen bonds start holding the structure together, which increases the tensile index of paper [44]. For machine made paper, the tensile load applied on the MD affects the extent of microcompression in the fibers aligned in this direction thus increasing their elastic modulus and tensile strength [1].

Dry lignin softens at 130°C to 190°C while dry hemicelluloses soften at 170 °C to 180°C [43]. As moisture content increases, the softening temperature of these two substances decreases. At the beginning of drying, the moisture content and temperature of the paper allow the lignin and hemicellulose to soften. This changes their structure from solid to plastic. The softened component of the fiber wall can form more hydrogen bonds [43], which improves the tensile strength of the paper. Lang, *et al.* [7] found that the high temperature drying of newsprint had no negative effect on the burst and tear indices. In addition, the Scott internal bond index remained constant, which proofed that higher temperature drying did not cause any delamination in paper strength.

EXPERIMENTAL SYSTEM

The experimental system used in this research was designed by Dr. John Cameron to simulate heat transfer into the paper during a typical paper cylinder drying process. Besides, the equipment simulates the drying process at elevated temperature represented by the GHPD. The system provides detailed information about the process and it is easy to change the input data from control variables such as shell temperature. Figure 4 shows a drawing by Dr. Cameron for the designed equipment. The system consists of a heated steel plate, a dryer fabric and thermocouples [34, 35].

A thermal heating pad manufactured by Heater Designs heats a one-half inch 304 stainless steel plate. The curvature of the steel shell is that of 2 m diameter dryers used in the industry. Paper is held against the metal shell by a permeable fabric under light pressure. The typical fabric tensions used in commercial dryer are 1.5 to 2.5 kN/m. From equation (4), the fabric tension was determined to be 1.1 kN/m, which is in the range recommended by TAPPI [45] for newsprint.

$$P=T/R \qquad (4)$$

Where P is the fabric pressure to hold the paper

T is the tension (kN/m).

R is the dryer cylinder radius (m).

Data are collected using three type E thermocouples and a temperature acquisition system manufactured by Computer Board Inc. The thermocouples are located in the paper, at the paper-heater interface and at the internal heater shell.

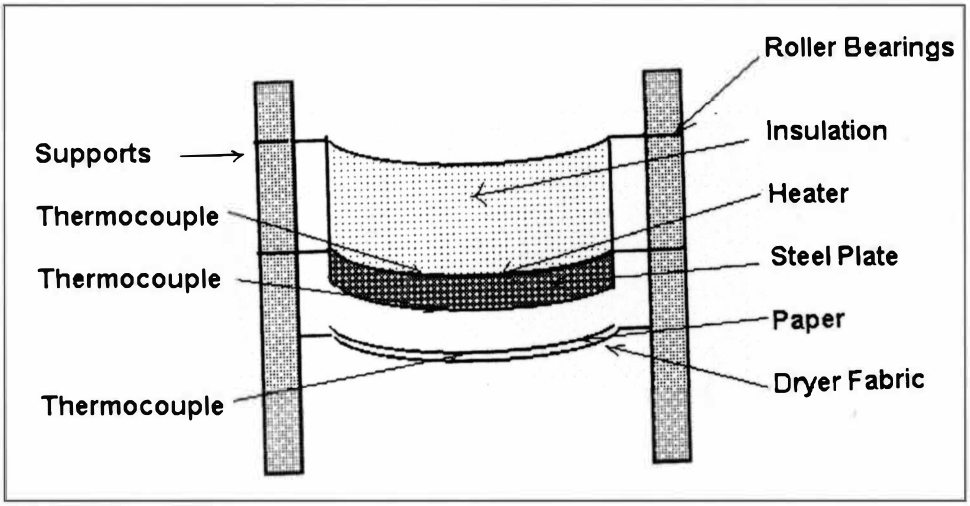

Figure 4. Experimental Paper Drying System Drawn by Dr. John Cameron [35].

The majority of the studies made on paper drying are focused on measuring the heat flux and shell-paper contact coefficient that has the most effect on drying. The thermocouples collected the three temperatures every 0.02 seconds. The collected data were then applied to an Explicit Finite difference method developed by Cameron [35] to calculate the heat flux. This method requires that the initial temperature of the metal surface be known and does not have to be uniform. Equation (5) presents a good development of the explicit finite difference method:

$$\frac{1}{\alpha'}\frac{\partial T}{\partial t} = \frac{\partial^2 T}{\partial x^2} + \frac{\partial^2 T}{\partial y^2} \qquad (5)$$

Where T is the temperature and x and y are the dimensions.

If the system is one dimensional in x, this equation can be written as an explicit form of a finite- difference equation as the following:

$$T_m^{p+1} = Fo\left(T_{m+1}^p + T_{m-1}^p\right) + \left(1 - 2Fo\right)T_m^p \qquad (6)$$

Where m is the dimensional subscript, p is the time subscript and $Fo = \alpha'\Delta t / \Delta x^2$ where Δt is the time interval and α' is the thermal diffusivity [46].

The heat flux model described above was written in Visual Basic™ for application to analyze the temperature of shell and paper surface. The Excel spreadsheet serves as an input-output platform for the program. Excel's chart feature can generate the required graphs. The calculated heat flux is then substituted in equation 1 to obtain the paper-shell contact coefficient. Handsheets were placed on the dryer fabric. As the heater was lowered onto the paper, the data acquisition program started collecting the data.

Experimental Conditions

Handsheets were made by using the Noble and Woods handsheet procedure from both softwood lap pulp and softwood lap pulp recycled one time.

The handsheets were dried at three shell temperatures (100 °C, 150 °C and 200 °C). The lowest temperature, 100 °C, corresponded to the average shell temperature used on conventional cylinder dryers producing newsprint. The highest temperature, 200°C, is representative of a gas heated dryer surface temperature [13].

In addition to the shell temperature and pulp type, other studied variables were basis weight, refining and moisture content. The three basis weights were 60g/m^2, 120 g/m^2 and 180 g/m^2. The pulp samples were refined by the Mead refiner for 15 seconds, 22.5 seconds and 30 seconds.

The wet handsheets were weighed before and after drying to check the moisture content and the amount of evaporated water. The moisture content of paper conveyed to a commercial drier is in the range 65% to 50% [8], which is around 2 to 1 g water/g oven dried fiber. To simulate the commercial drying conditions, the highest level of moisture content was 2 g H_2O/g dry fiber and the lowest was 1 g H_2O/g dry fiber. Appendix A shows the condition at each drying run.

Drying rates at the constant rate zone, first falling zone and second falling zone were analyzed at different process variables. The drying rate was obtained by dividing the amount of evaporated water over the drying time and the contact area between the sample and the heated plate. Appendix (Table A.1 and A.2) show the obtained drying rates and the contact coefficients at the constant rate zone, first falling rate zone and second falling rate zone.

The dried samples were tested for tensile strength according to TAPPI standard [47]. Appendix A (Table A.3) shows the average tensile indices for each run.

To study the effect of the high temperature drying on paper curl, the dried samples were cut into 15 mm width and 15 cm length strips. The samples were tested for curl then for tensile strength. Curl was determined from the angle of curvature of the edge rise and the distance between the edge and the midpoint of the strip [47]. The angle of curvature (θ) was calculated according to equation:

$$\theta = \tan^{-1} \Delta y/\Delta x \qquad (7)$$

where the angle (θ) and the dimensions x and y are shown in Figure 5.

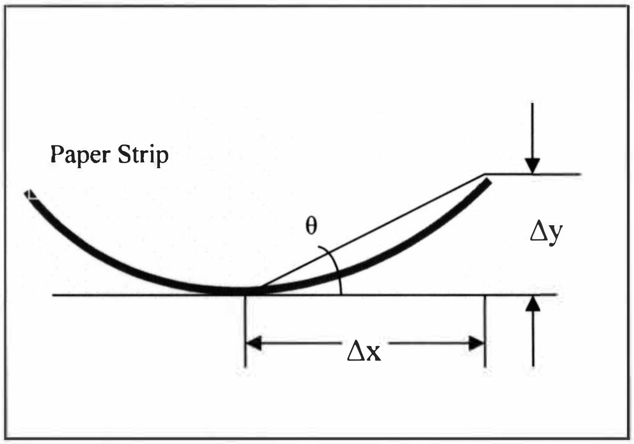

Figure 5: Curl Measurement for the Dried Paper Samples.

Humidity history of the dried samples is an important factor in curl measurement [47]. Therefore, the drying equipment, the dried samples and strips were kept under TAPPI standard conditions (25 ˚C and 50% humidity) while conducting all the experiments and measurements. Appendix A (Table A.4) shows the measured curl at each drying run.

RESULTS AND DISCUSSION

This research studied the effect of high surface temperature on the drying rate and the paper properties for both lap pulp and recycled paper. In addition, it provided information that optimized the location of a gas-fired paper dryer. The effect on the drying rate will be discussed first, followed by the effect on the contact coefficient and later on the sheet properties.

Although several drying experiments were conducted, only representative drying curves are presented. Appendix B shows sample figures for the drying rate and the contact coefficient. Figure 6 shows the temperature changes of the heated platen, paper and the heat flux into the sheet. As the shell contacts the sheet at the beginning of the drying, the temperature gradient between the two surfaces assists the heat transfer. The figure shows the increase of the paper temperature with this heat transfer until it reaches 100 °C. The water evaporates at this temperature and diffuses to the side away from the heated surface [25]. When the free water evaporates and the vapor flows directly to the air, the sheet temperature rises above 100 °C while the shell temperature decreases.

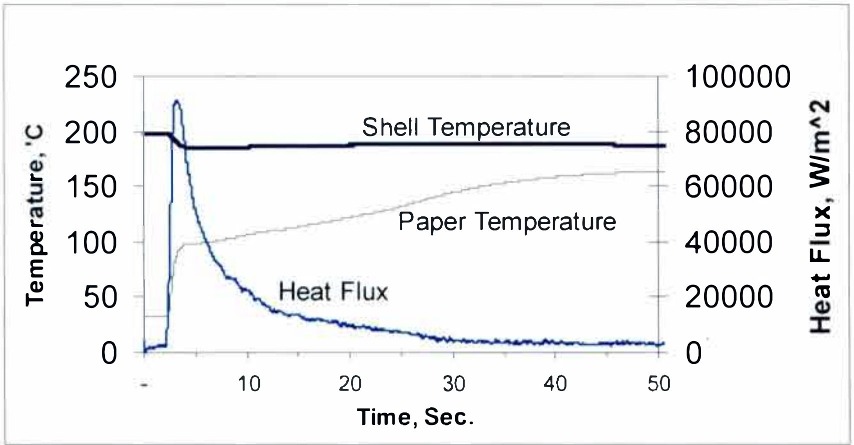

Figure 6. Heat Flux, Shell and Paper Temperatures for 120g/m^2 Lap Pulp at 200°C Shell Temperature.

The heat flux to the paper is directly related to the drying rate. Figure 7 and 8 show the drying curve and the distinct drying zones for softwood SW lap pulp and recycled paper. The first zone is the warm up zone where the drying rate increases continuously. The second zone is the constant rate zone. In this study, the second zone lasts for less than one second in all the drying experiments. The next zone is the first falling rate zone. The moisture content between the constant rate zone and the first falling zone is the critical moisture content. In the first falling zone, the surface of the web is partly dry and its heat conductivity decreases. This causes the web temperature to increase. The last zone is the bound water zone. In this zone, physicochemical bonds hold the remaining water. These bonds are difficult to break and this causes the drying rate to decrease.

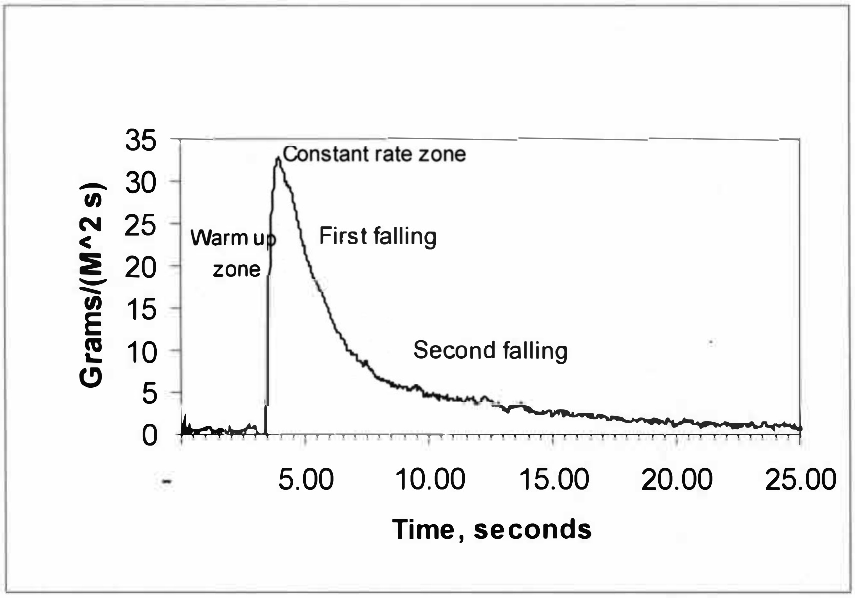

Figure 7. Drying Curve for Lap Pulp at 40% Solid Content, 180g/m^2 and 200°C Shell Temperature.

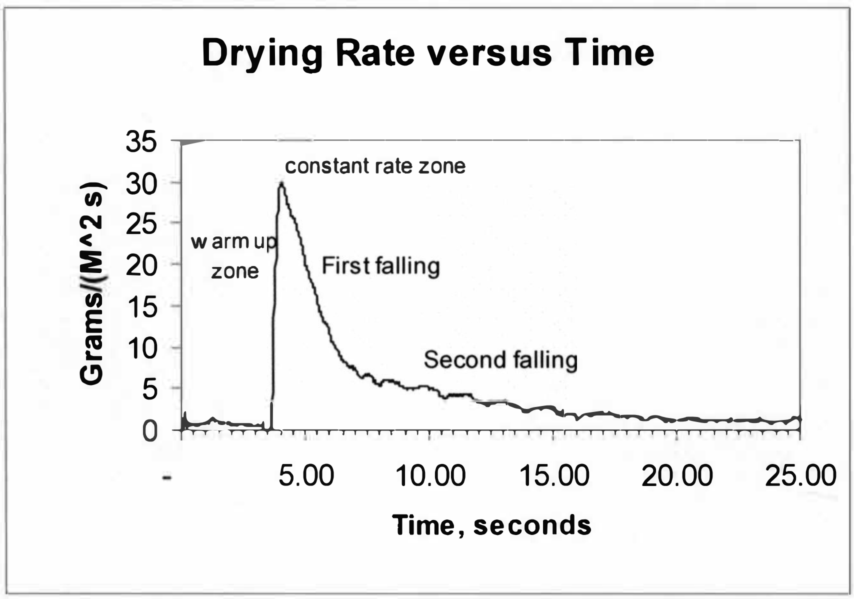

Figure 8. Drying Curve for Recycled Paper at 40% Solid Content, 180g/m^2 and 200°C Shell Temperature.

The data were analyzed by the Analysis of Variance method ANOVA MINITAB Release 14.1 [14] to determine the significant variable(s). Since there was more than one factor to investigate, the general linear model from ANOVA was applied. The response variable is the drying rate in the constant rate, the first falling rate and the second falling rate zones. Appendix C shows the analysis for the drying rates at 95% confidence interval (CI). Table 1 shows a summary of the p-values for the drying rates at the three drying zones.

Table 1. P-Values for Analysis of Variance for the Drying Rates

Factor	P-Value for Drying Rate in the Constant Rate Zone	P-Value for Drying Rate in the First Falling Rate Zone	P-Value for Drying Rate in the Second Falling Rate Zone
Recycling	0.078	0.226	0.225
Shell Temperature	0.000	0.000	0.000
Moisture Content	0.000	0.000	0.586
Refining	0.288	0.051	0.746

From table 1, it is obvious that both the temperature and the moisture content have the lowest p-values of all the factors. The temperature p-values (0.000) are smaller than the level of significance ($\alpha^* = 0.05$) in all the drying zones. Therefore, the mean drying rates in all the drying zones do differ significantly for higher temperatures. The p-values for the moisture effect were much smaller than α in the constant rate and the first falling rate zones while in the second falling rate zone the p-value was larger than α^*. Therefore, we cannot conclude that higher initial moisture content will give higher drying rates in all the drying zones. The obtained p-values for both recycling and refining were larger than 0.05. Therefore, we cannot reject the null hypothesis that the drying rates are the same for different levels of recycling and refining and these factors do not have a significant effect on the drying rates.

The scatter plot in Figures 9 to 11 agree with the statistical analysis. Figures 9 to 11 show the effect of shell temperature on the drying rate in the constant rate, first falling and second falling rate zones. As the shell temperature increases, the higher temperature difference between the shell and paper assists the heat transfer. The drying rate at the beginning of paper drying in the constant rate zone has the highest value compared with the first falling and the second falling zones. After the first falling zone, the paper is almost dry and sheet conductivity decreases. Therefore, the heat transfer decreases and the drying rate slow. As discussed earlier, paper recycling does not affect the drying rate in this study. In addition, the basis weight does not have any significant effect on paper drying rates in all the drying zones.

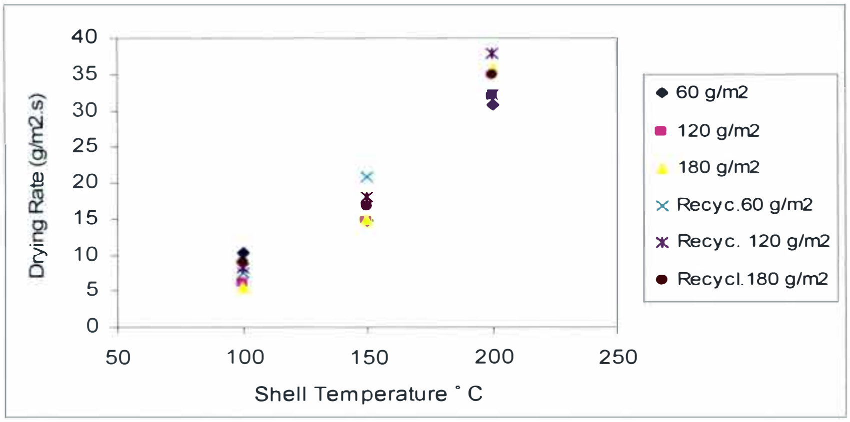

Figure 9. Effect of Shell Temperature and Basis Weight on the Drying Rate for Virgin Pulp and Recycled Paper in the Constant Rate Zone.

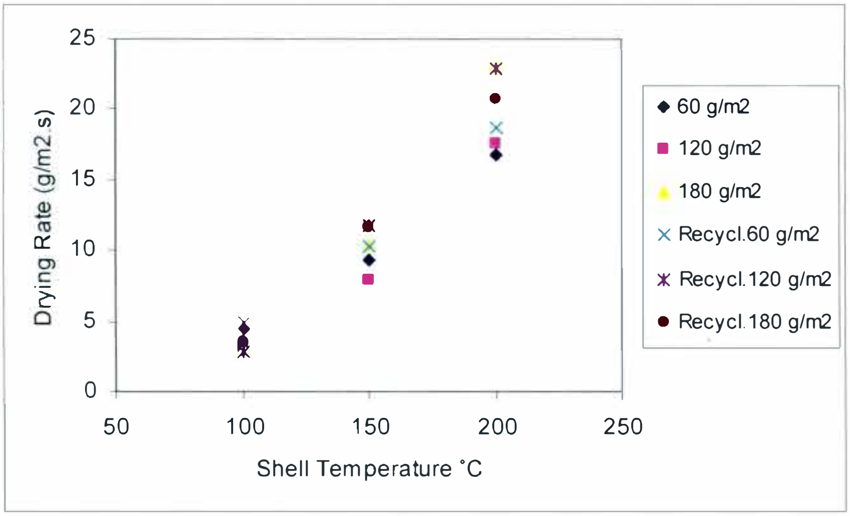

Figure 10. Effect of Shell Temperature and Basis Weight on the Drying Rate for Virgin Pulp and Recycled Paper in the First Falling Zone.

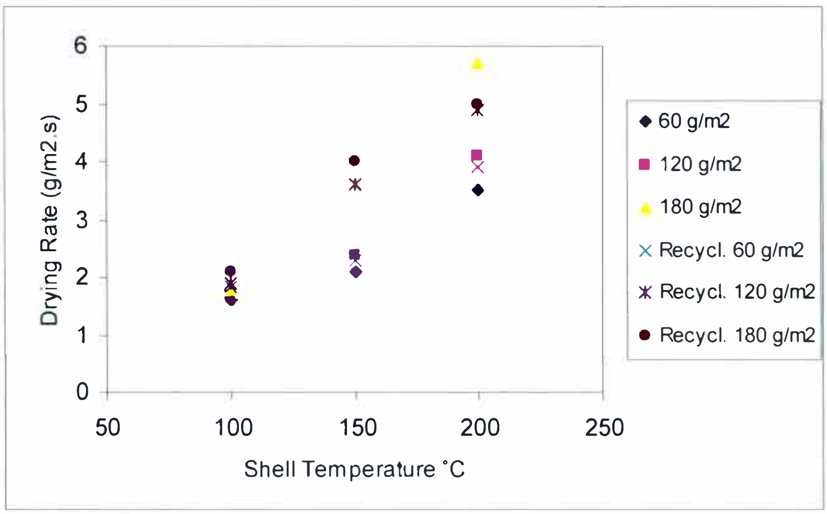

Figure 11. Effect of Shell Temperature and Basis Weight on the Drying Rate for Virgin Pulp and Recycled Paper in the Second Falling Zone.

Figure 12 shows the effect of moisture content on the average drying rates. The drying rates are the average for that of the three falling zones. Although the figure shows higher drying rates at 2 g/gOD moisture content, the values do not vary statistically.

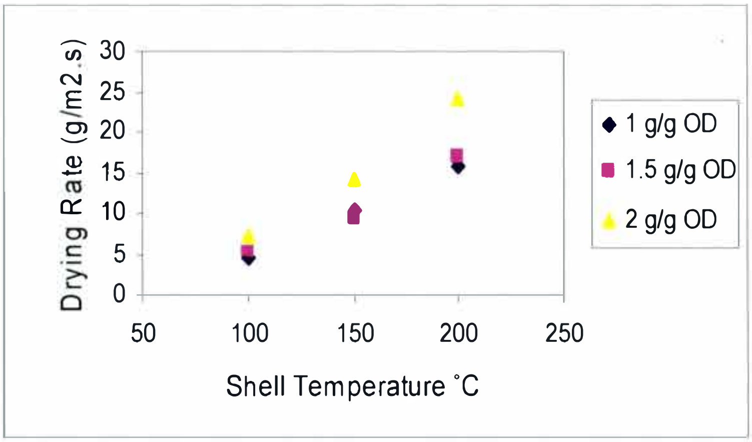

Figure 12. Effect of Moisture Content on the Average Drying Rates.

As discussed earlier, the heat transfer and hence the drying rate can be described by equation 1. The key resistance for paper drying is the contact coefficient between the dyer shell and the paper (α_k). The effect of high shell temperature on the contact coefficient in the literature was not clear and conflicting results were obtained. The statistical analysis in Appendix C showed large temperature p-values (for contact coefficient) than the level of significance (α^*) in the constant rate zone and first falling rate zones but a low temperature p-value than α^* in the second falling rate zone. Therefore, the shell-paper contact coefficient is independent on the shell temperature in the constant rate and first falling rate zones while it defers significantly with higher shell temperature in the second falling zone. Table 2 shows a summary of the p-values obtained by ANOVA.

Table 2. P-Values for Analysis of Variance for the Contact Coefficient

Factor	P-Value for Contact Coefficient in the Constant Rate Zone	P-Value for Contact Coefficient in the First Falling Rate Zone	P-Value for Contact Coefficient in the Second Falling Rate Zone
Recycling	0.043	0.099	0.609
Shell Temperature	0.595	0.011	0.000
Moisture Content	0.000	0.000	0.106
Refining	0.716	0.326	0.318

The low moisture contents' p-values show the dependency of the contact coefficient on the initial moisture content of the paper in both the constant and first falling zones. This can be explained by the higher contact between the shell and paper when paper is wet at beginning of drying. In the second falling zone, the paper is almost dry and the initial moisture content of paper had no effect on the contact coefficient in this zone.

Figures 13,14 and 15 agree with the above results where the paper-shell contact coefficient was independent on the shell temperature neither in the constant drying rate zone and in the first following rate zone, but decreased with temperature in the second following rate zone. This may be due to the physical-chemical bonding of the water to the fibers that must be overcome in the second following rate region. The analysis also shows that both the soft wood (SW) lap pulp and the recycled pulp behaved similarly with regard to the effect of the shell temperature on this contact effect. In addition, the contact coefficient does not vary with different basis weights in all figures.

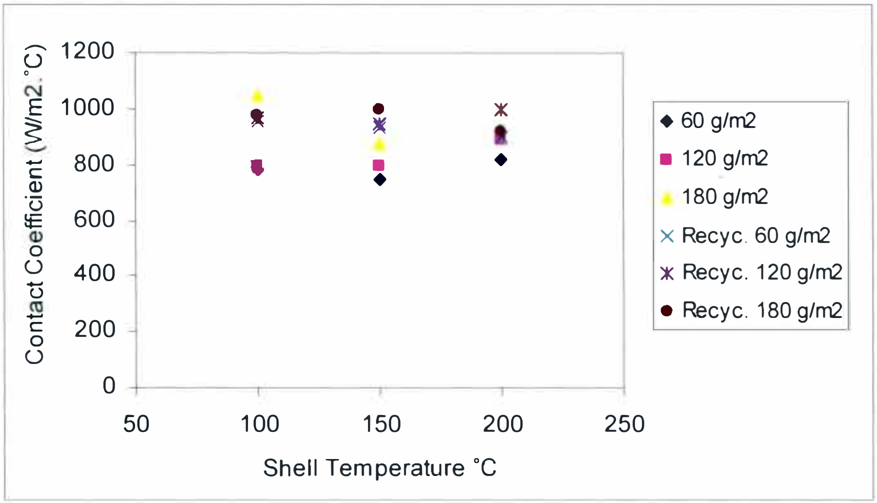

Figure 13. Effect of Shell Temperature and Basis Weight on the Contact Coefficient for Lap Pulp and Recycled Paper in the Constant Rate Zone.

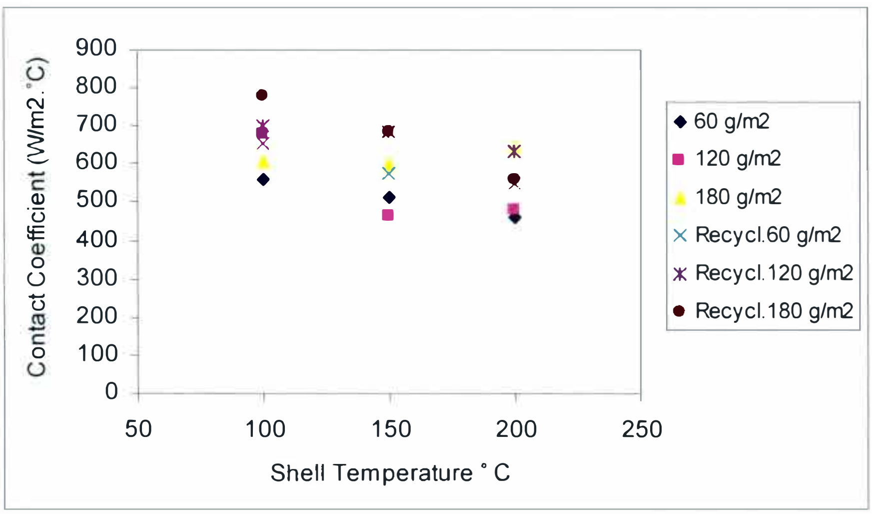

Figure 14. Effect of Shell Temperature and Basis Weight on the Contact Coefficient for Lap Pulp and Recycled Paper in the First Falling Zone.

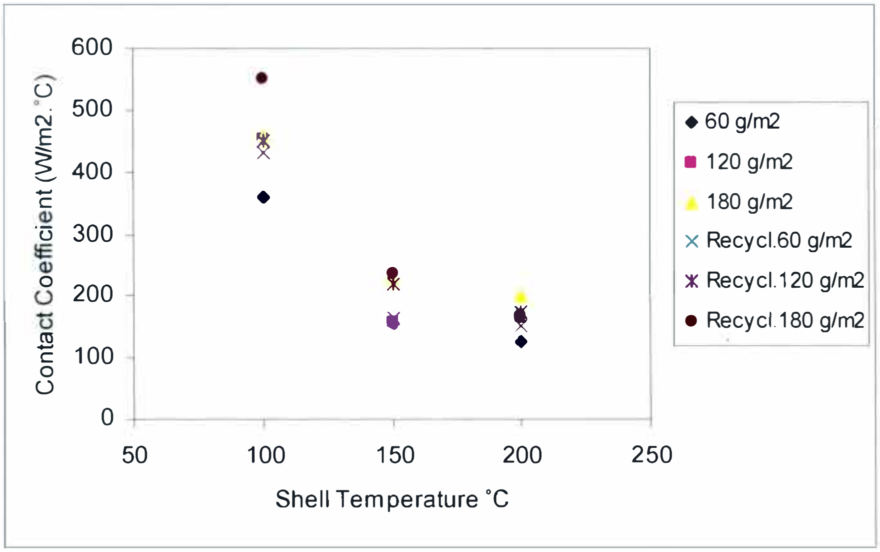

Figure 15. Effect of Shell Temperature and Basis Weight on the Contact Coefficient for Lap Pulp and Recycled Paper in the Second Falling Zone.

With the above finding, we are able to predict the ideal location of a high temperature dryer. If the high temperature dryer is placed in the beginning of the drying chain toward the wet end, a vapor film will form between the shell and the paper that acts as a barrier to the heat transfer. If it is placed too far toward the dry end, it will be located in the second following rate zone where the contact coefficient decreases at high shell temperatures. Therefore, the heat transfer rate and hence drying rate will not increase as fast with an increase in shell temperature. Therefore, the ideal location for the high shell dryer should be in the middle of the dryer chain and both the beginning and the end should be avoided.

In the middle of the dryer chain, the high temperature dryer will be located within the constant rate or first falling rate zone. The heat transfer rate can be described by equation (1) in these zones with α_k remaining relatively constant and not affected with high shell temperature.

With a gas fired dryer, the shell temperature can be as high as 300 °C while the highest shell temperature with conventional steam drying is about 150 °C. Therefore, the high temperature dryer provides higher temperature difference between the shell and paper. According to equation 1, an increase in the temperature difference (ΔT) – the driving force for the drying process- increases the heat transfer and hence the drying rates. The results show about three times increase in the drying rate as the shell temperature increases from 150 °C to 200 °C for each high temperature dryer added. With such a temperature, there are some concerns with the use of a high temperature felt and the fire safety systems on the dryer. However, two or three times an increase in heat transfer and drying rate should be attainable.

This research also examined the effect of pulp refining on the contact coefficient. The statistical analysis in Appendix C and the high refining p-values in Table 2 showed that the refining level had no significant effect on the contact coefficient. The results in Figures 16 to 18 agree with this finding. The figures represent the results obtained for $60 g/m^2$ handsheets at 1.5 g/g OD initial moisture content in the three drying zones.

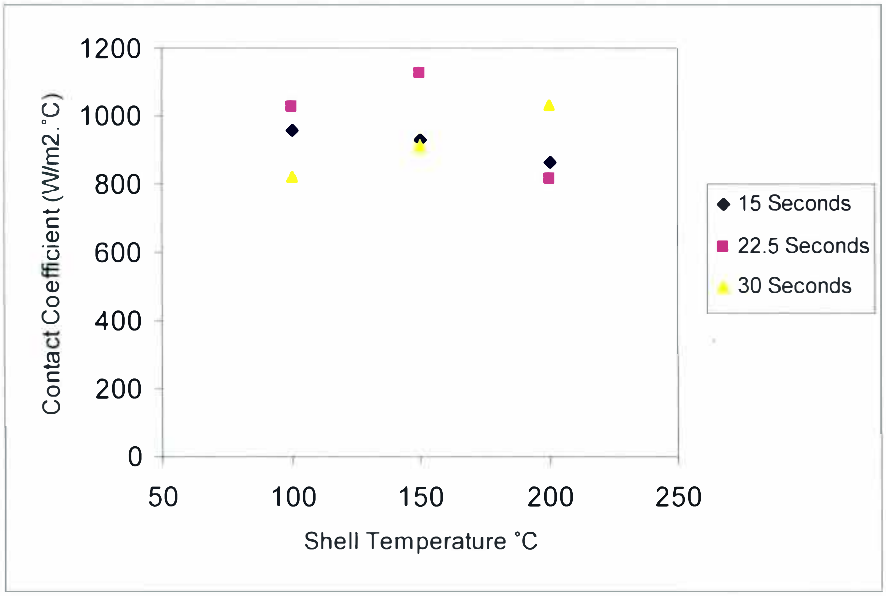

Figure 16. Effect of Shell Temperature and Refining on the Contact Coefficient for Recycled Paper in the Constant Rate Zone.

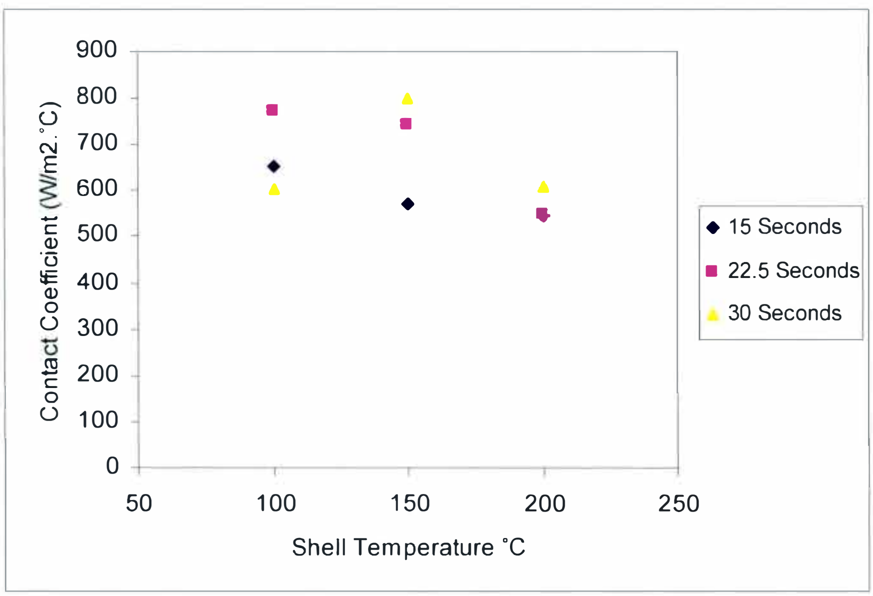

Figure 17. Effect of Shell Temperature and Refining on the Contact Coefficient for Recycled Paper in the First Falling Rate Zone.

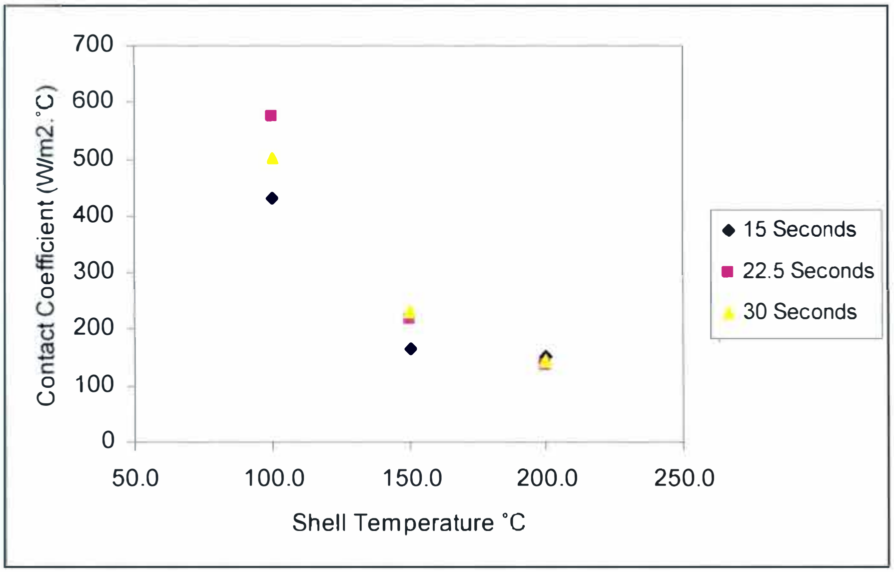

Figure 18. Effect of Shell Temperature and Refining on the Contact Coefficient for Recycled Paper in the Second Falling Rate Zone.

Another aspect of high temperature drying is the effect on paper properties. Tensile strength was measured for all the dried samples and two-way ANOVA was applied to determine the effect of high temperature drying and recycling on paper strength. The statistical analysis in Appendix C showed that paper strength was not affected by shell temperature while decreased with paper recycling. This decrease in the tensile strength of recycled paper could be explained as the reduction of fiber-fiber bonding strength with recycling. Figure 19 shows two-sided 95% confidence intervals on the means for both the recycling and the temperature effects. From the overlap of the tensile indices means intervals with different shell temperatures, we can conclude that the shell temperature has no negative effect on paper strength.

```
                  Individual 95% CIs For Mean Based on
                  Pooled StDev
Pulp      Mean   -------+---------+---------+---------+--
Lap      16.6967                    (---------*----------)
Recycled  13.9570  (---------*---------)
                 -------+---------+---------+---------+--
                     13.5      15.0      16.5      18.0


                         Individual 95% CIs For Mean Based on
                         Pooled StDev
Temperature      Mean   -----+---------+---------+---------+----
100           14.6692   (------------*-----------)
150           15.1619       (-----------*------------)
200           16.1496             (------------*-----------)
                        -----+---------+---------+---------+----
                           13.5      15.0      16.5      18.0
```

Figure 19. Confidence Intervals on the Mean of Tensile Indices.

The scatter plot in Figure 20 agrees with the statistical analysis where the high shell temperature does not affect paper strength. The result in this figure represents the tensile index value for 60 g/m^2, 120 g/m^2, and 180 g/m^2 handsheets dried at 1.5 g/g initial moisture content at 15 seconds refining.

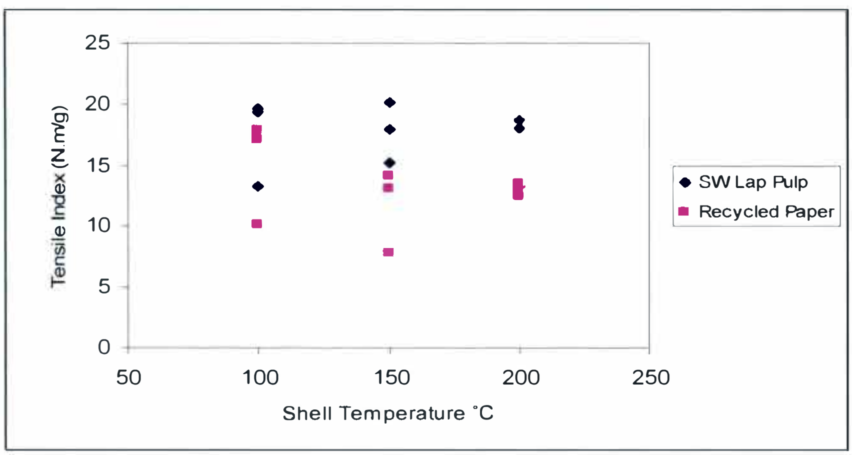

Figure 20. Effect of Shell Temperature and Recycling on Average Paper Tensile Index.

To study the effect of the high temperature gas-heated driers on paper curl, the dried samples were cut into 15 mm width and 15 cm length strips. Curl was determined from the angle of curvature of the edge rise and the distance between the edge and the midpoint of the strip. As expected, the dried papers curled away from the heated surface toward the side dried last. Figure 21 shows different paper curl at high temperatures for lap pulp and recycled paper. The results show higher paper curl with higher temperatures for lap SW pulp. While for recycled paper, this result is not observed and it is clear that recycling reduces paper tendency to curl. The statistical analysis at 95% confidence interval in Appendix C supports the above discussion where the obtained p-values were 0.001 and 0.000 for both the effect of recycling and shell temperature respectively. Therefore, both paper recycling and high shell temperatures affect paper tendency to curl.

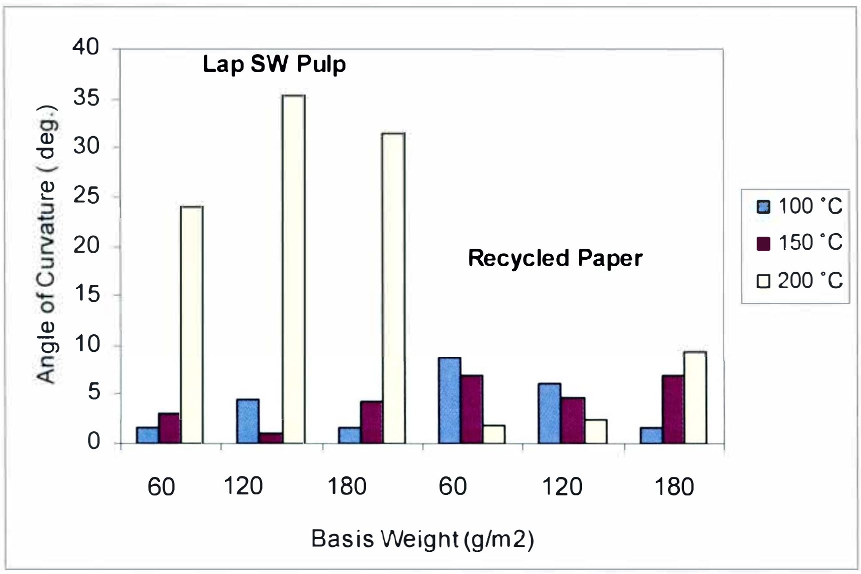

Figure 21. Effect of Shell Temperature on Paper Curl.

Fibers swelling and shrinkage after drying could explain the observed reduction of paper curl with recycling treatment. The drying and re-wetting cycles and recycling treatment reduce the re-swelling capability of chemical pulp fibers by affecting the hydrogen bonding and crystallinity of fiber walls [51, 52]. Therefore, fibers swell less with recycling and less shrinkage and hence less curl are obtained.

The above results showed the effect of high shell temperature on paper curl and curl direction. However, the curl resulted from all the heat transfer from one side of the paper. In a commercial operation, paper curl would be less and curl tendency could be counteracted with a single high temperature drying. If the machine situation changed due factors such as furnish changes or machine speed, a problem could be rise where paper would curl. Ideally, at least two high temperature dryer should be installed. This would control any increase in paper curl by adjusting the relative temperature of the two high temperature dryers.

CONCLUSIONS

This research examined two important aspects of high temperature paper drying applications. These aspects are the effect of the high surface temperature on the drying rate and paper properties. In addition, the results helped to identify the ideal location of the high temperature dryers.

Statistical analysis of the results provided information about the significant factor in this research. Shell temperature was the significant variable that affected the drying rate in all the drying zones and the contact coefficient in the second falling zone. With a gas fired drying, the shell temperature can be as high as 300 °C, which provides higher temperature difference between the paper and the shell to increase the drying rates by 2 to 4 % in all the drying zones.

The paper-shell contact coefficient was not affected by shell temperature in either the constant rate zone and in the first following rate zone. While in the second falling rate zone, the contact coefficient decreased with higher shell temperatures. This decrease was present for both lap pulp and recycled paper. Based on this result, the high temperature dryer should be installed in the middle and both the beginning and the end of the dryer chain should be avoided.

The effect of paper moisture content on the contact coefficient supports the above conclusion. As the moisture content of the paper increases, the contact coefficient increases in both the constant rate and the first falling rate zones. In the second falling zone, the moisture content does not affect the contact coefficient. This can be explained by the direct contact between the shell and paper at higher moisture contents. Therefore, to achieve higher contact coefficients and hence higher drying rates, the high temperature dryer should be installed in the middle of the dryer and avoid the beginning and the end of the dryer.

Both the basis weight and pulp refining did not affect the contact coefficients and the drying rates of the paper.

The main consideration about the installation of high temperature drying is the effect on paper properties. Results on paper tensile indices do not show any significant effect of this high temperature on paper strength. Therefore, there are no evidence on a negative effect of high shell temperature on paper strength for both lap pulp and recycled paper.

The high temperature and especially one side drying affected paper curl. In all cases, the paper tended to curl away from the heated side toward the side heated last. The curling tendency was less in recycled paper than that of lap pulp.

To avoid the curling tendency of paper at high temperature drying, the gas-heated dryer should be installed such that it counteracts paper curl. Ideally, at least two high temperature dryer should be installed to control this high curl tendency by adjusting the relative temperature between the two dryers.

REFERENCES

1- Peel, J. D. (1992) *Paper Science and Paper Manufacture.* Angus Wild Publications, Inc. (pp 192).

2- Karlsson, M. (2000) *Papermaking Part 2.* Drying Papermaking Science and Technology Book 9, TAPPI Press (pp: 92).

3- Smook, G.A. (1992) *Handbook for Pulp and Paper Technologists.* Angus Wild Publications, Inc. (pp. 264).

4- Gas-Fired Infrared Paper Drying. The Energy Solution Center's Consortium Website. Retrieved February 16, 2007 from http://www.energysolutionscenter.org/GasIRPaper/WhyGasIR.htm

5-Chudnovsky, Y. Innovative Gas-Fired Technology for Paper Drying. 2004 TAPPI Paper Summit Spring Technical and International Environmental Conference: May 3-5, 2004, Atlanta, GA USA (pp: 709- 712).

6- Karlsson, M. (2000) *Papermaking Part 2.* Drying Papermaking Science and Technology Book 9, TAPPI Press (pp: 333).

7-Lang, I., Smith, R., Tawfik, and Poirier, N.A. (2001) *High Temperature Gas-Heated Drying Cylinders: Potential Impact on Drying Rate and Product Quality.* Pulp and Paper Canada, 102 (3) (pp: 34- 39).

8- Peel, J. D. (1992) *Paper Science and Paper Manufacture.* Angus Wild Publications, Inc. (pp 171).

9- Smook, G.A. (1992) *Handbook for Pulp and Paper Technologists.* Angus Wild Publications, Inc. (pp. 267).

10- Peel, J. D. (1992) *Paper Science and Paper Manufacture.* Angus Wild Publications, Inc. (pp 175).

11- Smook, G.A. (1992) *Handbook for Pulp and Paper Technologists.* Angus Wild Publications, Inc. (pp. 265).

12- Karlsson, M. (2000) *Papermaking Part 2.* Drying Papermaking Science and Technology Book 9, TAPPI Press (pp: 111).

13-Poirier, D. (1994). High Surface Temperature Paper and Board Drying. *Paper Makers Conference TAPPI Proceedings* (pp: 547-552).

14-British Gas - Patent Application WO 99/45196.

15-ABB Drying - US Patent 5,791,065.

16-Gastec NV - US Patent 5,842,285.

17-GTI - US Patent 6,877,979

18-- Laboratory Development of High-Capacity, Gas-Fired Paper Dryer Forest. Project Fact Sheet Website. Retrieved December 21, 2007 from http://www1.eere.energy.gov/industry/forest/pdfs/gasfired_dryer.pdf

19- Gas Fired Paper dryer John Wozny.

20- GTI - US Patent 6,877,979.

21- Karlsson, M. (2000) *Papermaking Part 2.* Drying Papermaking Science and Technology Book 9, TAPPI Press (pp: 62- 63).

22- Karlsson, M. (2000) *Papermaking Part 2.* Drying Papermaking Science and Technology Book 9, TAPPI Press (pp: 334).

23-Alkhasawneh, H., and Cameron, J. H. Effect of Fiber Fractionation on Sheet Properties and Drying Behavior. TAPPI Engineering, Pulping, Environmental Conference, Philadelphia, PA 2005.

24- Molnar, K. (1987) Handbook of Industrial drying in A.S. Mujumdar, (Ed.), Marcel Dekker, NY.

25-- Peel, J. D. (1992) *Paper Science and Paper Manufacture.* Angus Wild Publications, Inc. (pp 181).

26- Smook, G.A. (1992) *Handbook for Pulp and Paper Technologists.* Angus Wild Publications, Inc. (pp. 266).

27- Karlsson, M. (2000) *Papermaking Part 2.* Drying Papermaking Science and Technology Book 9, TAPPI Press (pp: 107).

28-Wilhelmsson, B., Fagerholm, L., Nilsson, L., and Strenstom, S., Tappi, 77(5) 159 (1994).

29- C-Redfern, A.P., The Paper Maker145 (6): 57 (1963).

30- Karlsson, M. (2000) *Papermaking Part 2.* Drying Papermaking Science and Technology Book 9, TAPPI Press (pp: 1110).

31- Karlsson, M. (2000) *Papermaking Part 2.* Drying Papermaking Science and Technology Book 9, TAPPI Press (pp: 61).

32-Hinds, J. and Neogi, A., TAPPI J. 66(6): 79 (1983).

33- Karlsson, M. (2000) *Papermaking Part 2.* Drying Papermaking Science and Technology Book 9, TAPPI Press (pp: 108).

34-Cameron, J. and Tripathi, P., 12th International Drying Symposium "Measurement of Paper-Shell Contact Coefficients".

35-Cameron, J. H., and Zwick T. R. A., The Effect of Fiber Recycling on Paper Drying 2003 TAPPI Spring Technical Conference & Trade Fair.

36- Yamagishi, Y., Japan TAPPI, v. 35, no. 9, Sept 9 (1981).

37- Karlsson, M. (2000) *Papermaking Part 2.* Drying Papermaking Science and Technology Book 9, TAPPI Press (pp: 337- 338).

38- Peel, J. D. (1992) *Paper Science and Paper Manufacture.* Angus Wild Publications, Inc. (pp 51- 52).

39- Niskanen, K., (1998) *Paper Physics*, Fapetoy Finland Publication, (pp: 37-40).

40 - Karlsson, M. (2000) *Papermaking Part 2.* Drying Papermaking Science and Technology Book 9, TAPPI Press (pp: 351- 353).

41- Niskanen, K., (1998) *Paper Physics*, Fapetoy Finland Publication, (pp: 223- 235).

42-Siegel, R. and Howell, J.R., (1981) *Thermal Radiation Heat Transfer*, 2nd E d., Hemispherer Publishing Corp., New York.

43 - Karlsson, M. (2000) *Papermaking Part 2.* Drying Papermaking Science and Technology Book 9, TAPPI Press (pp: 339- 348).

44-Nordman, L., Levlin, J-E., and Visti, J., Kuivatuksen Vaikutus Paperirainan Ominaisuuksiin. Paperin valmistus, osa 1. Ed. Arjas, A. *SPIY/TTA*, Turku 1983 (in Finnish).

45-TAPPI Technical Information Sheets, (1989) vol. 1: Series 0100-0300: 0404, Recommended Tension for Dryer Felts.

46-Dewitt, D.P., (1985) *Introduction to Heat Transfer*, Transient Conduction. John Wiley & Sons, Inc., (pp: 173-242).

47-Mark, R. E., Habeger, C. C., Borch, J., and Lyne M. B. (Eds) (2002) *Handbook of Physical Testing of Paper.* Vol (1) 2nd Ed., Marcel Dekker, Inc., (pp: 160- 163).

48-TAPPI Standard Method- TAPPI T494.

49-Meet MINITAB Statistical Software Release 13 for Windows®, Minitab Inc., Feb. 2002.

50- Khantayanuwong, S. (2002) *Effects of Beating and Recycling on Strength of Pulp Fibers and Paper*, Kasetsart J. (Nat. Sci.), (pp: 193-199).

51- Jang, H. F., R. C. Howard, and R. S. Seth. (1995). Fiber Characterization Using Confocal Microscopy-The Effects of Recycling. Tappi J. 78 (12) (pp: 131-137).

52- Khantayanuwong, S., T. Enomae, A. Isogai, and F. Onabe. (2002). Changes in Crystallinity and Reswelling Capability of Pulp Fibers by Recycling Treatment. Japan Tappi J. 56 (6) (pp: 863-869).

Appendix A

Estimated Values of Responses

TABLE A.1: CONTACT COEFFICIENT ESTIMATION

Control Variables						Response Variables		
Run #	Pulp Type	Shell Temperature (°C)	Moisture Content (g/g OD)	Refining (seconds)	Basis Wight (g/m^2)	Contact Coefficient in Constant Rate Zone ($W/m^2.°C$)	Contact Coefficient in First Falling Rate Zone ($W/m^2.°C$)	Contact Coefficient in Second Falling Rate Zone ($W/m^2.°C$)
1-1	R	100	1.5	15.0	60	1067.91	609.0	427.0
1-2	R	100	1.5	15.0	60	843.94	694.0	438.0
2-1	R	150	1.5	15.0	60	886.48	573.0	159.0
2-2	R	150	1.5	15.0	60	976.33	590.0	171.0
3-1	R	200	1.5	15.0	60	932.42	580.0	166.0
3-2	R	200	1.5	15.0	60	798.70	514.0	138.0
4-1	R	100	1.5	15.0	120	700.00	450.0	300.0
4-2	R	100	1.5	15.0	120	710.00	455.0	320.0
5-1	R	150	1.5	15.0	120	1111.07	685.0	217.0
5-2	R	150	1.5	15.0	120	1069.12	688.0	225.0
6-1	R	200	1.5	15.0	120	974.51	634.0	172.0
6-2	R	200	1.5	15.0	120	1214.03	670.0	178.0
7-1	R	100	1.5	15.0	180	1043.05	780.0	550.0
7-2	R	100	1.5	15.0	180	1040.00	800.0	557.0
8-1	R	150	1.5	15.0	180	912.62	622.0	222.0
8-2	R	150	1.5	15.0	180	1120.95	748.0	251.0
9-1	R	200	1.5	15.0	180	1020.61	594.0	183.0
9-2	R	200	1.5	15.0	180	817.53	525.0	157.0
10-1	L	100	1.5	15.0	60	1056.22	725.0	369.0
10-2	L	100	1.5	15.0	60	1006.94	473.0	350.0
11-1	L	150	1.5	15.0	60	547.37	380.0	129.0
11-2	L	150	1.5	15.0	60	825.70	650.0	185.0

TABLE A.1- Continued

Run #	Pulp Type	Shell Temperature (°C)	Moisture Content (g/g OD)	Refining (seconds)	Basis Wight (g/m^2)	Contact Coefficient in Constant Rate Zone (W/m^2.°C)	Contact Coefficient in First Falling Rate Zone (W/m^2.°C)	Contact Coefficient in Second Falling Rate Zone (W/m^2.°C)
12-1	L	200	1.5	15.0	60	775.83	497.0	127.0
12-2	L	200	1.5	15.0	60	862.39	426.5	129.0
13-1	L	100	1.5	15.0	120	771.22	620.0	420.0
13-2	L	100	1.5	15.0	120	798.57	736.0	489.0
14-1	L	150	1.5	15.0	120	775.00	405.4	159.2
14-2	L	150	1.5	15.0	120	826.00	487.0	170.5
15-1	L	200	1.5	15.0	120	944.66	549.0	168.0
15-2	L	200	1.5	15.0	120	838.76	481.0	160.0
16-1	L	100	1.5	15.0	180	792.29	610.0	395.0
16-2	L	100	1.5	15.0	180	752.13	609.0	518.0
17-1	L	150	1.5	15.0	180	994.01	632.0	232.0
17-2	L	150	1.5	15.0	180	758.67	575.0	229.0
18-1	L	200	1.5	15.0	180	1209.97	602.0	183.0
18-2	L	200	1.5	15.0	180	903.60	703.0	222.0
19-1	L	100	1.0	15.0	60	722.00	539.0	342.0
19-2	L	100	1.0	15.0	60	618.00	424.0	245.0
20-1	L	150	1.0	15.0	60	705.00	613.0	229.0
20-2	L	150	1.0	15.0	60	708.00	602.0	215.0
21-1	L	200	1.0	15.0	60	711.00	407.0	120.0
21-2	L	200	1.0	15.0	60	727.00	417.0	120.0
22-1	L	100	2.0	15.0	60	900.00	714.0	432.0
22-2	L	100	2.0	15.0	60	1413.00	995.0	600.0
23-1	L	150	2.0	15.0	60	1085.00	847.0	226.0
23-2	L	150	2.0	15.0	60	1316.00	884.0	201.0

TABLE A.1- Continued

Run #	Pulp Type	Shell Temperature (˚C)	Moisture Content (g/g OD)	Refining (seconds)	Basis Wight (g/m^2)	Contact Coefficient in Constant Rate Zone (W/m^2.˚C)	Contact Coefficient in First Falling Rate Zone (W/m^2.˚C)	Contact Coefficient in Second Falling Rate Zone (W/m^2.˚C)
24-1	L	200	2.0	15.0	60	1153.00	645.0	131.0
24-2	L	200	2.0	15.0	60	1191.00	672.0	154.0
25-1	R	100	1.5	22.5	60	1187.00	912.0	660.0
25-2	R	100	1.5	22.5	60	866.00	634.0	493.0
26-2	R	150	1.5	22.5	60	1223.00	816.0	233.0
26-2	R	150	1.5	22.5	60	1041.00	676.0	206.0
27-1	R	200	1.5	22.5	60	816.00	550.0	138.0
27-2	R	200	1.5	22.5	60	816.00	550.0	138.0
28-1	R	100	1.5	30.0	60	822.00	606.0	503.0
28-2	R	100	1.5	30.0	60	822.00	606.0	503.0
29-1	R	150	1.5	30.0	60	914.00	800.0	235.0
29-2	R	150	1.5	30.0	60	914.00	800.0	235.0
30-1	R	200	1.5	30.0	60	1100.00	650.0	150.0
30-2	R	200	1.5	30.0	60	966.00	566.0	142.0

TABLE A.2: DRYING RATE ESTIMATION

Run #	Pulp Type	Shell Temperature (˚C)	Moisture Content (g/g OD)	Refining (seconds)	Basis Wight (g/m^2)	Drying Rate in Constant Rate Zone ($g/m^2.s$)	Drying Rate in First Falling Rate Zone ($g/m^2.s$)	Drying Rate in Second Falling Rate Zone ($g/m^2.s$)
1-1	R	100	1.5	15.0	60	13.0190	4.40	1.90
1-2	R	100	1.5	15.0	60	9.3357	5.30	1.80
2-1	R	150	1.5	15.0	60	24.2419	10.30	2.30
2-2	R	150	1.5	15.0	60	22.1104	10.60	2.50
3-1	R	200	1.5	15.0	60	34.7166	21.00	4.30
3-2	R	200	1.5	15.0	60	29.5882	16.50	3.50
4-1	R	100	1.5	15.0	120	2.9400	1.46	1.00
4-2	R	100	1.5	15.0	120	2.9900	1.45	1.10
5-1	R	150	1.5	15.0	120	18.2539	11.80	3.60
5-2	R	150	1.5	15.0	120	18.1859	11.90	3.60
6-1	R	200	1.5	15.0	120	36.5578	23.00	4.90
6-2	R	200	1.5	15.0	120	43.4673	22.90	5.00
7-1	R	100	1.5	15.0	180	5.3872	3.60	2.10
7-2	R	100	1.5	15.0	180	5.5000	3.50	2.00
8-1	R	150	1.5	15.0	180	15.0850	10.90	3.80
8-2	R	150	1.5	15.0	180	18.4630	12.40	4.10
9-1	R	200	1.5	15.0	180	35.4552	21.80	5.15
9-2	R	200	1.5	15.0	180	30.3364	19.70	5.00
10-1	L	100	1.5	15.0	60	10.4200	4.79	1.57
10-2	L	100	1.5	15.0	60	10.2200	4.12	1.62
11-1	L	150	1.5	15.0	60	14.3000	10.00	1.59
11-2	L	150	1.5	15.0	60	15.2000	12.17	2.70

TABLE A.2- Continued

Run #	Pulp Type	Shell Temperature (°C)	Moisture Content (g/g OD)	Refining (seconds)	Basis Wight (g/m^2)	Drying Rate in Constant Rate Zone ($g/m^2.s$)	Drying Rate in First Falling Rate Zone ($g/m^2.s$)	Drying Rate in Second Falling Rate Zone ($g/m^2.s$)
12-1	L	200	1.5	15.0	60	30.8000	18.10	2.30
12-2	L	200	1.5	15.0	60	31.2000	15.20	3.50
13-1	L	100	1.5	15.0	120	5.4941	3.50	1.70
13-2	L	100	1.5	15.0	120	7.1180	3.00	1.60
14-1	L	150	1.5	15.0	120	13.8000	7.20	2.20
14-2	L	150	1.5	15.0	120	14.4000	8.00	2.40
15-1	L	200	1.5	15.0	120	34.0689	20.20	4.60
15-2	L	200	1.5	15.0	120	30.1290	17.60	4.10
16-1	L	100	1.5	15.0	180	5.3609	3.10	1.70
16-2	L	100	1.5	15.0	180	5.5220	3.00	1.80
17-1	L	150	1.5	15.0	180	16.0690	10.90	3.40
17-2	L	150	1.5	15.0	180	13.1287	10.20	3.80
18-1	L	200	1.5	15.0	180	41.2799	21.82	5.30
18-2	L	200	1.5	15.0	180	30.2177	24.60	6.55
19-1	L	100	1.0	15.0	60	8.2000	4.31	1.07
19-2	L	100	1.0	15.0	60	8.2600	4.63	1.35
20-1	L	150	1.0	15.0	60	18.2200	12.47	4.04
20-2	L	150	1.0	15.0	60	16.3800	11.67	3.92
21-1	L	200	1.0	15.0	60	27.6000	15.44	3.20
21-2	L	200	1.0	15.0	60	28.6700	15.77	3.42
22-1	L	100	2.0	15.0	60	14.7000	4.22	1.65
22-2	L	100	2.0	15.0	60	14.9000	6.47	2.45
23-1	L	150	2.0	15.0	60	24.1600	14.92	3.74
23-2	L	150	2.0	15.0	60	24.4700	14.89	3.24

TABLE A.2- Continued

Run #	Pulp Type	Shell Temperature (˚C)	Moisture Content (g/g OD)	Refining (seconds)	Basis Wight (g/m^2)	Drying Rate in Constant Rate Zone (g/m^2.s)	Drying Rate in First Falling Rate Zone (g/m^2.s)	Drying Rate in Second Falling Rate Zone (g/m^2.s)
24-1	L	200	2.0	15.0	60	43.2700	23.80	3.63
24-2	L	200	2.0	15.0	60	44.5400	24.69	4.75
25-1	R	100	1.5	22.5	60	11.6000	6.80	2.40
25-2	R	100	1.5	22.5	60	9.4300	4.85	1.79
26-2	R	150	1.5	22.5	60	21.4200	15.10	3.70
26-2	R	150	1.5	22.5	60	21.3800	12.43	3.47
27-1	R	200	1.5	22.5	60	31.2000	18.80	3.40
27-2	R	200	1.5	22.5	60	31.2000	18.80	3.40
28-1	R	100	1.5	30.0	60	8.1000	4.60	1.90
28-2	R	100	1.5	30.0	60	8.1000	4.60	1.90
29-1	R	150	1.5	30.0	60	20.2000	15.30	4.10
29-2	R	150	1.5	30.0	60	20.2000	15.30	4.10
30-1	R	200	1.5	30.0	60	43.5000	24.60	4.30
30-2	R	200	1.5	30.0	60	37.2400	20.75	3.87

TABLE A.3: TENSILE INDEX AND ANGLE OF CURVATURE

Run #	Pulp Type	Shell Temperature (˚C)	Moisture Content (g/g OD)	Refining (seconds)	Basis Wight (g/m^2)	Tensile Index (N.m/g)	Angle of Curvature (˚)
1-1	R	100	1.5	15.0	60	10.0995	2.2000
1-2	R	100	1.5	15.0	60	9.6172	6.5000
2-1	R	150	1.5	15.0	60	7.7756	5.7000
2-2	R	150	1.5	15.0	60	7.8629	5.2000
3-1	R	200	1.5	15.0	60	12.6966	4.5000
3-2	R	200	1.5	15.0	60	12.0432	2.5000
4-1	R	100	1.5	15.0	120	6.0000	3.0000
4-2	R	100	1.5	15.0	120	6.3000	1.5600
5-1	R	150	1.5	15.0	120	14.4984	2.0000
5-2	R	150	1.5	15.0	120	13.6056	7.8000
6-1	R	200	1.5	15.0	120	13.1700	8.0000
6-2	R	200	1.5	15.0	120	13.3878	9.4000
7-1	R	100	1.5	15.0	180	17.4342	9.3300
7-2	R	100	1.5	15.0	180	16.4856	1.5500
8-1	R	150	1.5	15.0	180	13.2747	2.0000
8-2	R	150	1.5	15.0	180	12.4822	2.3370
9-1	R	200	1.5	15.0	180	9.5785	3.9000
9-2	R	200	1.5	15.0	180	11.5512	25.0000
10-1	L	100	1.5	15.0	60	12.2665	23.4800
10-2	L	100	1.5	15.0	60	14.2918	3.8700
11-1	L	150	1.5	15.0	60	15.4297	4.4600
11-2	L	150	1.5	15.0	60	13.4806	1.3200

TABLE A.3- Continued

Run #	Pulp Type	Shell Temperature (˚C)	Moisture Content (g/g OD)	Refining (seconds)	Basis Wight (g/m^2)	Tensile Index (N.m/g)	Angle of Curvature (˚)
12-1	L	200	1.5	15.0	60	13.1811	0.7690
12-2	L	200	1.5	15.0	60	13.1430	31.0000
13-1	L	100	1.5	15.0	120	19.0173	37.5700
13-2	L	100	1.5	15.0	120	19.3821	2.3400
14-1	L	150	1.5	15.0	120	20.7486	1.5000
14-2	L	150	1.5	15.0	120	19.6162	5.0000
15-1	L	200	1.5	15.0	120	19.2950	4.2300
15-2	L	200	1.5	15.0	120	18.0155	30.2000
16-1	L	100	1.5	15.0	180	19.8104	31.8000
16-2	L	100	1.5	15.0	180	18.4347	0.7660
17-1	L	150	1.5	15.0	180	13.6981	0.8450
17-2	L	150	1.5	15.0	180	14.0683	30.9600
18-1	L	200	1.5	15.0	180	19.7414	31.5500
18-2	L	200	1.5	15.0	180	18.0827	37.4500
19-1	L	100	1.0	15.0	60	10.6590	45.0000
19-2	L	100	1.0	15.0	60	9.8120	4.6470
20-1	L	150	1.0	15.0	60	17.5120	3.0940
20-2	L	150	1.0	15.0	60	18.5790	7.9100
21-1	L	200	1.0	15.0	60	19.9320	7.8500
21-2	L	200	1.0	15.0	60	21.2520	3.0900
22-1	L	100	2.0	15.0	60	15.0920	3.8600
22-2	L	100	2.0	15.0	60	14.7620	1.9168
23-1	L	150	2.0	15.0	60	23.5950	2.0000
23-2	L	150	2.0	15.0	60	20.9660	13.0000

TABLE A.3- Continued

Run #	Pulp Type	Shell Temperature (˚C)	Moisture Content (g/g OD)	Refining (seconds)	Basis Wight (g/m^2)	Drying Rate in Constant Rate Zone ($g/m^2.s$)	Drying Rate in First Falling Rate Zone ($g/m^2.s$)
24-1	L	200	2.0	15.0	60	13.8710	11.0000
24-2	L	200	2.0	15.0	60	13.1670	10.5200
25-1	R	100	1.5	22.5	60	12.3750	11.0000
25-2	R	100	1.5	22.5	60	13.8820	1.5430
26-2	R	150	1.5	22.5	60	13.5300	1.0000
26-2	R	150	1.5	22.5	60	13.5520	3.8700
27-1	R	200	1.5	22.5	60	18.6890	3.9200
27-2	R	200	1.5	22.5	60	19.2280	3.1200
28-1	R	100	1.5	30.0	60	23.5400	4.6860
28-2	R	100	1.5	30.0	60	24.1230	2.2000
29-1	R	150	1.5	30.0	60	13.3760	6.5000
29-2	R	150	1.5	30.0	60	15.5870	5.7000
30-1	R	200	1.5	30.0	60	20.2290	5.2000
30-2	R	200	1.5	30.0	60	22.7370	4.5000

TABLE A.4: AVERAGE DIMENSIONS FOR THE STRIPS IN CALCUALTING THE ANGLE OF CURVATURE (θ) FOR FIGURE 29

Run #	Pulp Type	Shell Temperature (˚C)	Moisture Content (g/g OD)	Refining (seconds)	Basis Wight (g/m^2)	x (cm)	y (cm)	tan θ = y/x	θ (˚)
1	R	100	1.5	15.0	60	7.33	1.13	0.16	8.80
2	R	150	1.5	15.0	60	7.30	0.90	0.12	7.03
3	R	200	1.5	15.0	60	7.36	0.25	0.03	1.93
4	R	100	1.5	15.0	120	7.20	0.75	0.11	6.00
5	R	150	1.5	15.0	120	7.35	0.60	0.08	4.69
6	R	200	1.5	15.0	120	7.30	0.30	0.04	2.35
7	R	100	1.5	15.0	180	7.35	0.20	0.027	1.56
8	R	150	1.5	15.0	180	7.30	1.00	0.14	7.80
9	R	200	1.5	15.0	180	7.28	1.20	0.16	9.36
10	L	100	1.5	15.0	60	7.40	0.20	0.03	1.55
11	L	150	1.5	15.0	60	7.32	0.40	0.06	3.12
12	L	200	1.5	15.0	60	6.10	2.65	0.43	23.48
13	L	100	1.5	15.0	120	7.38	0.58	0.08	4.46
14	L	150	1.5	15.0	120	7.43	0.12	0.02	0.95
15	L	200	1.5	15.0	120	6.80	1.37	0.70	35.3
16	L	100	1.5	15.0	180	7.37	0.2	0.03	1.57
17	L	150	1.5	15.0	180	7.23	0.53	0.07	4.23
18	L	200	1.5	15.0	180	5.80	3.55	0.62	31.51
19	L	100	1.0	15.0	60	7.45	0.11	0.02	0.84
20	L	150	1.0	15.0	60	6.03	3.10	0.52	27.16
21	L	200	1.0	15.0	60	4.57	4.20	0.92	42.48
22	L	100	2.0	15.0	60	7.26	0.93	0.13	7.39
23	L	150	2.0	15.0	60	7.22	1.07	0.15	8.41
24	L	200	2.0	15.0	60	7.4	0.52	0.07	3.99
25	R	100	1.5	22.5	60	7.45	0.22	0.03	2.00
26	R	150	1.5	22.5	60	7.18	1.40	0.20	11.00

TABLE A.4- Continued

Run #	Pulp Type	Shell Temperature (˚C)	Moisture Content (g/g OD)	Refining (seconds)	Basis Wight (g/m^2)	x (cm)	y (cm)	tan θ = y/x	θ (˚)
27	R	200	1.5	22.5	60	7.07	1.37	0.19	11.00
28	R	100	1.5	30.0	60	7.43	0.17	0.02	1.00
29	R	150	1.5	30.0	60	7.33	0.57	0.08	4.00
30	R	200	1.5	30.0	60	7.32	0.67	0.09	5.00

Appendix B

Sample Figures Obtained From Excel Spreadsheet

***Run 15-1:**

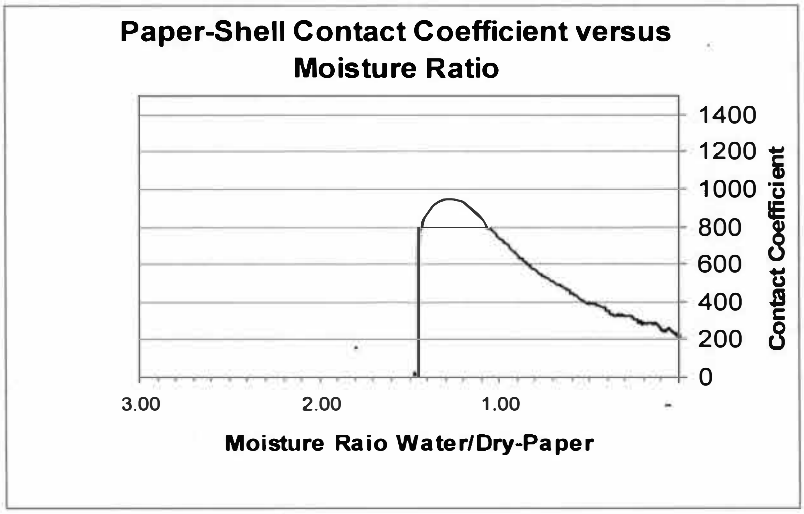

Figure 31. Shell Paper Contact Coefficient at 1.5 g/g OD Initial Moisture Content for Run # 15-1.

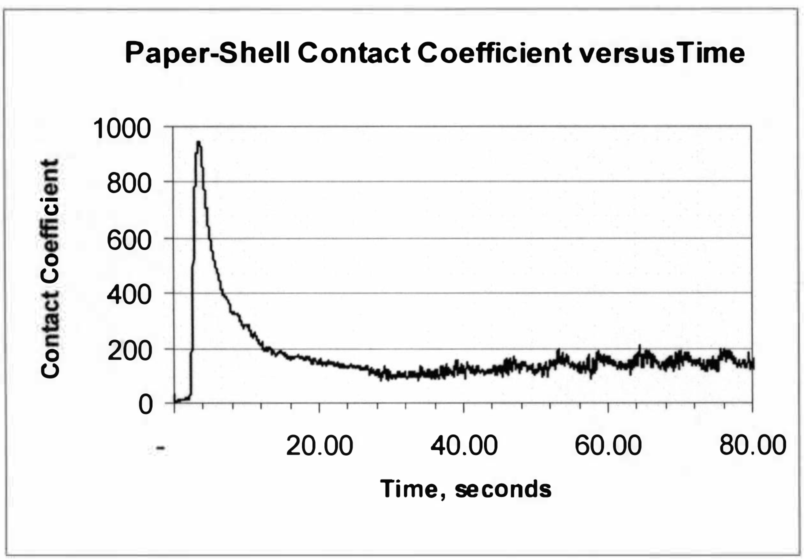

Figure 32. Shell Paper Contact Coefficient for Run # 15-1.

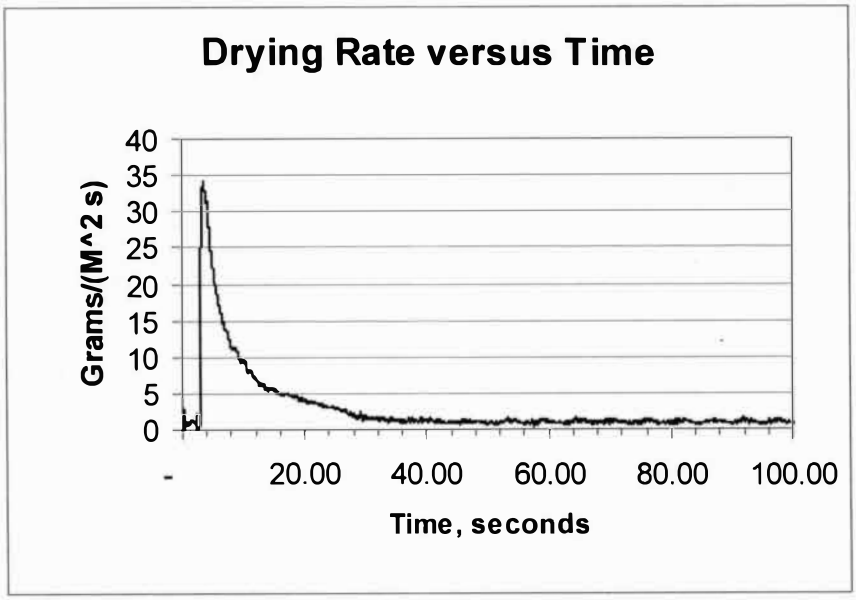

Figure 33. Drying Rate for Run # 15-1.

Appendix C

Statistical Analysis By Minitab Release 14.1

General Linear Model: Drying Rate-, Drying Rate-, ... versus Pulp, Temperature,

```
Factor              Type    Levels  Values
Pulp                fixed        2  L, R
Temperature         fixed        3  100, 150, 200
Moisture Content    fixed        3  1.0, 1.5, 2.0
Refining            fixed        3  15.0, 22.5, 30.0


Analysis of Variance for Drying Rate-Constant Rate Zone, using Adjusted SS
for
     Tests

Source              DF   Seq SS   Adj SS   Adj MS       F      P
Pulp                 1     12.2     37.8     37.8    3.23  0.078
Temperature          2   7105.9   7105.9   3552.9  303.26  0.000
Moisture Content     2    434.2    434.2    217.1   18.53  0.000
Refining             2     29.9     29.9     15.0    1.28  0.288
Error               52    609.2    609.2     11.7
Total               59   8191.5


S = 3.42283   R-Sq = 92.56%   R-Sq(adj) = 91.56%


Unusual Observations for Drying Rate-Constant Rate Zone

            Drying
      Rate-Constant
Obs       Rate Zone      Fit   SE Fit  Residual  St Resid
 12         43.4673  34.5431  1.0205     8.9242      2.73 R
 35         41.2799  32.4928  1.0205     8.7871      2.69 R
 59         43.5000  37.1202  1.5307     6.3798      2.08 R

R denotes an observation with a large standardized residual.


Analysis of Variance for Drying Rate-First Falling Zone, using Adjusted SS
for
     Tests

Source              DF   Seq SS   Adj SS   Adj MS       F      P
Pulp                 1     9.33     6.26     6.26    1.50  0.226
Temperature          2  2615.02  2615.02  1307.51  313.88  0.000
Moisture Content     2    74.20    74.20    37.10    8.91  0.000
Refining             2    26.35    26.35    13.18    3.16  0.051
Error               52   216.61   216.61     4.17
Total               59  2941.51


S = 2.04100   R-Sq = 92.64%   R-Sq(adj) = 91.64%


Unusual Observations for Drying Rate-First Falling Zone
```

Obs	Drying Rate-First Falling Zone	Fit	SE Fit	Residual	St Resid
24	15.2000	19.1387	0.6085	-3.9387	-2.02 R
36	24.6000	19.1387	0.6085	5.4613	2.80 R

R denotes an observation with a large standardized residual.

Analysis of Variance for Drying Rate-Second Falling Zone, using Adjusted SS for Tests

Source	DF	Seq SS	Adj SS	Adj MS	F	P
Pulp	1	0.8378	0.7569	0.7569	1.32	0.255
Temperature	2	63.5667	63.5667	31.7833	55.59	0.000
Moisture Content	2	0.6178	0.6178	0.3089	0.54	0.586
Refining	2	0.3372	0.3372	0.1686	0.29	0.746
Error	52	29.7309	29.7309	0.5717		
Total	59	95.0904				

S = 0.756141   R-Sq = 68.73%   R-Sq(adj) = 64.53%

Unusual Observations for Drying Rate-Second Falling Zone

Obs	Drying Rate-Second Falling Zone	Fit	SE Fit	Residual	St Resid
21	1.59000	3.14661	0.22544	-1.55661	-2.16 R
23	2.30000	4.04011	0.22544	-1.74011	-2.41 R
36	6.55000	4.04011	0.22544	2.50989	3.48 R

R denotes an observation with a large standardized residual.

General Linear Model: Contact Coef, Contact Coef, ... versus Pulp, Temperature,

Factor	Type	Levels	Values
Pulp	fixed	2	L, R
Temperature	fixed	3	100, 150, 200
Moisture Content	fixed	3	1.0, 1.5, 2.0
Refining	fixed	3	15.0, 22.5, 30.0

Analysis of Variance for Contact Coefficient-Constant Ra, using Adjusted SS for Tests

Source	DF	Seq SS	Adj SS	Adj MS	F	P
Pulp	1	69220	89995	89995	4.30	0.043
Temperature	2	21912	21912	10956	0.52	0.595
Moisture Content	2	730681	730681	365341	17.47	0.000
Refining	2	14078	14078	7039	0.34	0.716
Error	52	1087505	1087505	20914		
Total	59	1923397				

```
S = 144.615   R-Sq = 43.46%   R-Sq(adj) = 35.85%


Unusual Observations for Contact Coefficient-Constant Ra

                  Contact
     Coefficient-Constant
Obs                    Ra      Fit  SE Fit  Residual  St Resid
 21                547.37   869.63   43.12   -322.26     -2.33 R
 35               1209.97   872.81   43.12    337.16      2.44 R
 44               1413.00  1149.37   64.67    263.63      2.04 R

R denotes an observation with a large standardized residual.


Analysis of Variance for Contact Coefficient-First Falli, using Adjusted SS
for
     Tests

Source            DF   Seq SS   Adj SS   Adj MS      F      P
Pulp               1    35386    30631    30631   2.81  0.099
Temperature        2   108134   108134    54067   4.97  0.011
Moisture Content   2   305187   305187   152593  14.02  0.000
Refining           2    24952    24952    12476   1.15  0.326
Error             52   566118   566118    10887
Total             59  1039776


S = 104.340   R-Sq = 45.55%   R-Sq(adj) = 38.22%


Unusual Observations for Contact Coefficient-First Falli

               Contact
     Coefficient-First
Obs              Falli      Fit  SE Fit  Residual  St Resid
  7            450.000  650.768  31.108  -200.768     -2.02 R
 21            380.000  596.549  31.108  -216.549     -2.17 R
 49            912.000  717.602  46.662   194.398      2.08 R

R denotes an observation with a large standardized residual.


Analysis of Variance for Contact Coefficient-Second Fall, using Adjusted SS
for
     Tests

Source            DF   Seq SS   Adj SS   Adj MS       F      P
Pulp               1    11133     1070     1070    0.27  0.609
Temperature        2   966972   966972   483486  119.89  0.000
Moisture Content   2    18924    18924     9462    2.35  0.106
Refining           2     9458     9458     4729    1.17  0.318
Error             52   209699   209699     4033
Total             59  1216186


S = 63.5033   R-Sq = 82.76%   R-Sq(adj) = 80.44%


Unusual Observations for Contact Coefficient-Second Fall

                Contact
```

Obs	Coefficient-Second Fall	Fit	SE Fit	Residual	St Resid	
7	300.000	445.327	18.933	-145.327	-2.40	R
8	320.000	445.327	18.933	-125.327	-2.07	R
38	245.000	388.772	28.400	-143.772	-2.53	R
44	600.000	467.605	28.400	132.395	2.33	R
49	660.000	488.272	28.400	171.728	3.02	R

R denotes an observation with a large standardized residual.

Two-way ANOVA: Tensile Index versus Pulp, Temperature

Source	DF	SS	MS	F	P
Pulp	1	112.59	112.589	6.45	0.014
Temperature	2	22.73	11.365	0.65	0.525
Interaction	2	46.13	23.066	1.32	0.275
Error	54	942.51	17.454		
Total	59	1123.96			

S = 4.178   R-Sq = 16.14%   R-Sq(adj) = 8.38%

```
                   Individual 95% CIs For Mean Based on
                   Pooled StDev
Pulp      Mean     -------+---------+---------+---------+--
L      16.6967                       (----------*----------)
R      13.9570     (----------*---------)
                   -------+---------+---------+---------+--
                        13.5      15.0      16.5      18.0
```

```
                            Individual 95% CIs For Mean Based on
                            Pooled StDev
Temperature      Mean       -----+---------+---------+---------+----
100           14.6692       (------------*-----------)
150           15.1619           (-----------*------------)
200           16.1496                 (------------*-----------)
                            -----+---------+---------+---------+----
                                13.5      15.0      16.5      18.0
```

Two-way ANOVA: Curl versus Pulp, Temperature

Source	DF	SS	MS	F	P
Pulp	1	812.49	812.487	13.42	0.001
Temperature	2	1728.17	864.087	14.28	0.000
Interaction	2	1452.28	726.138	12.00	0.000
Error	54	3268.61	60.530		
Total	59	7261.55			

S = 7.780   R-Sq = 54.99%   R-Sq(adj) = 50.82%

```
                   Individual 95% CIs For Mean Based on
                   Pooled StDev
Pulp      Mean     --+---------+---------+---------+-------
L      12.9783                            (-------*-------)
R       5.6185     (-------*-------)
                   --+---------+---------+---------+-------
```